We thank reviewers for their comments and suggestions. Our point-by-point reply to these comments is below.

Referee #1 comments:

I have one major point, where I do not understand the results of the model simulations: It is not clear to me, why in the model the peak of the stratospheric sulfate burden is reached only five months after the eruption (see also below). I strongly suggest a more detailed discussion of this point, which without further explanation looks like a model artifact to the reader.
// *It is not clear to me, why in the model the peak of the stratospheric sulfate burden is reached 5 months after the eruption. I can understand how this could be the case for the HIRS observations, where the initial plume has to be diluted somewhat to be properly quantified by measurements. But I do not think that such a behaviour is seen in Lidar observations of the Pinatubo cloud. In the model however there is no substantial source of stratospheric sulphur after the eruption. The only process I can see is the conversion of SO2 to sulfate, but the timescale for this to happen should be much less than five months. I suggest more discussion of this point.//*

As the referee commented, the only process that contributes to stratospheric sulfate burden is the conversion of the SO2 to sulfate, and this will take some time and depend e.g. on the OH concentration at a specific location. Roughly 80% of SO2 is oxidized after three months after the eruption (see Figure A2). The oxidation rate in the NH (i.e. which during the eruption is the summer hemisphere with abundant OH) is fast in the months following the eruption, and but slows down considerably during the winter months (Fig. A2a; months ~4-8). As a result, the NH peak burden is reached at around month 3 and then declines very slowly until around month 6. On the other hand, in the SH (i.e. during the eruption in the winter hemisphere), the peak burden is reached only in late spring (~month 5) when the OH concentration has increased as a response to increased solar radiation. As a result, also the global burden peaks around month 5.

Text is now modified:
"The maximum stratospheric sulfate burden after the volcanic eruption (Volc) is 8.31 Tg(S). 75% of the erupted SO_2 is oxidized in two months after the eruption, mostly in the summer hemisphere (NH). However some of the SO_2 is spread to the winter hemisphere (SH) where OH concentration in the first months following the eruption is low due to lower solar radiation. As the OH abundance in the SH increases towards spring, the peak burden in this hemisphere is reached around month 5 (Fig. A2b). As a result, also the global maximum of sulfate burden is reached 5 months after the eruption (Fig. 2a, black solid line)."

It is stated in the paper that under unperturbed conditions, the atmosphere is "almost clean" of particles. I think this is an overstatement. First, it is unclear under which conditions the stratosphere is really unperturbed, i.e. not influenced by small volcanic eruptions. Second, OCS provides a source of sulphur to the stratosphere. Therefore there will always be a Junge layer in the stratosphere, so that "clean" is misleading.
We admit that "clean" is a bit misleading here. Thus "Clean" is now replaced by "unperturbed".

In any case, there is no reference here for this statement Volcanic ash emissions are not taken into account in the study. The argument is that ash particles are deposited fast. However the citation (Niemeier et al., 2009) used to back up this conclusion is a model study, I recommend considering a study based on observations. For example, the eruption of the Chilean volcano Puyehue-Cordón Caulle in June 2011 emitted a lot of ash that prevailed long enough in the atmosphere to cause interruption of passenger aircraft activity in Australia. In any case, it is not the question how much sulphur is contained in volcanic ash (close to zero) but how much sulphur is emitted in conjunction with the ash. The sulphur contribution is not the same for each eruption – again there should be observational studies here.

It is true that volcanic ash could have some impact on air traffic. However only fine ash particles reach the stratosphere. Larger particles stay in the troposphere but have an impact on aviation and health. Guo et al 2004a have shown that volcanic ash is sediments within the first days after the Mt.Pinatube eruption. Less the 5% of the erupted ash was detected in the stratosphere after 5 days the resulting ash cloud is typically fairly local and short-lived. Also previous model studies (Niemeier et al. 2009) and our test simulations showed that volcanic ash does not affect conclusions related to emitted sulfur. Because of these reasons, and because we wanted to keep study as simplified as possible, we decide to leave volcanic ash out of this study.

Reference (Guo et al 2004) is now added in the text:

"We do not include volcanic ash emissions as it has been shown that ash is deposited relatively fast in the atmosphere and the surface area affected by the ash cloud is relatively small (Guo et al 2004a). The effect of fine ash on the distribution of the volcanic cloud in the atmosphere is also relatively small (Niemeier et al 2009)."

The dynamical feedback from the increased stratospheric sulphur load was taken into account. I think this is an interesting point of the study. Could the authors present some discussion on this point?
Dynamical feedback is taken account, but it is very difficult to identify how this has affected the our results without making an extensive additional analysis, which is out of the scope of this study. We have added:

"*However global aerosol model studies of the Pinatubo eruption (Timmreck et al 1999; Aquial et al 2013) showed that the dynamic response to local aerosol heating has an important influence on the initial dispersal of the volcanic cloud. Performing non-interactive and interactive Pinatubo simulations these studies revealed that an interactive coupling of the aerosol with the radiation scheme is necessary to adequately describe the observed transport characteristics over the first months after the eruption. Only the interactive model simulations where the volcanic aerosol is seen by the radiation scheme are able to simulate the observed initial southward cross-equatorial transport of the cloud as well as the aerosol lifting to higher altitudes. A further improvement of the interactive simulation is a reduced northward transport and an enhanced meridional transport towards the south, which is consistent with satellite observations."*

There is some discussion on the differences between MPI-ESM and the SALSA aerosol treatment and the consequences for the radiative effects. Is there a reference to a study, where these differences have been investigated? Can "somewhat different radiative forcing" be quantified? How well does the scaling to other wavelengths work? Would the scattering radius be a better quantity to use than the effective radius? I suggest further discussion of these issues.
Unfortunately there is no reference study for our treatment of aerosol radiative properties. We admit that scaling to the other wavelengths is not unproblematic, as this leads to some overestimation on both SW and LW radiative forcings. The overestimation is larger for LW radiation which in our case leads to about 0.65 W/m2 smaller global mean aerosol radiative forcing in ESM for SRM scenario. However, this does not impact the conclusions of our study. Even though there is some difference between the models in their calculated radiative effect of stratospheric aerosol, there are many uncertainties in the model which cause much larger uncertainty in aerosol radiative effects. Adding to this, the aerosol forcing is affected also by other things that impact radiation in atmosphere such as surface albedo or cloud properties which could be quite different between a model which includes a

coupled ocean model and a model that uses fixed sea surface temperature. Most relevantly, we do not directly compare the results from ECHAM-HAM and ESM. All scenarios are compared against scenarios from the same model. Furthermore, the general conclusions which were made for aerosol radiative effects from the ECHAM-HAM simulations, also hold for simulations with MPI-ESM.

Text in the section 3.3 is rewritten:
"This in turn leads to an overestimation of the longwave radiative forcing (0.7 W/m^2 for SRM) while the shortwave forcing is less affected (-0.2 W/m^2 for SRM)."

HIRS does not directly observe the stratospheric sulphur burden (p. 21864). I think a bit more information on the satellite measurements should be given here. How do the HIRS values agree with other observations?
We are not aware of a proper comparison between HIRS and the other measurements. Also the lack of measurements of SO4 burden makes comparison difficult. HIRS instrument was originally designed for vertical sounding of humidity and temperature profiles and was not ideally for stratospheric sulfate measurements.

Some studies (Guo et al 2004b and Bluth et al 1992) have estimated that the initial SO2 mass was 18-20 Mt (9-10 Tg(S)) after the eruption. As mentioned earlier, this was oxidized to sulfate in a few months after the eruption. Based on the HIRS measurements, maximum sulfate burden was lower than 6 Tg(S) which implicates much smaller initial SO2 mass or that large proportion of sulfur mass was removed from the atmosphere first few months after eruption.

Please not that after our manuscript was submitted, we found out that there is a mistake in the figure caption of Baran and Foot (1994). Whereas the caption states that figure shows burden of H2SO4, in reality the figure shows shows mixture of (75% H2SO4 and 25% H2O). This decreases our values from HIRS data by 25%"

How is the sulphur lifetime in the stratosphere defined? Burden over loss rate? This quantity could also be a function of time. I suggest further discussion.
For SRM lifetime is calculated as Burden/Injected sulfur. For volcanic eruptions we do not quantify lifetime, because, as the referee pointed out, it would be a function of time and thus difficult to define. The text now reads: "The total sulfur amount (SO_2 and sulfate) in the stratosphere is 8.8 Tg(S) which indicates the average sulfur lifetime (*sulfur burden divided by the amount of the injected sulfur*).."

There is some discussion of the oxidation of SO2 in the model (p. 21860). If there is something problematic in the model here, it will have to do with the OH concentrations in the model – correct? Is there any information on the quality of OH in the model from previous studies? OH is a pretty important component in atmospheric chemistry.

We are not aware of a proper validation of quality of OH in the model. In the model OH based on monthly mean values with artificial diurnal cycle. Pietikäinen et al 2012 (Atmos. Chem. Phys., 14, 11711-11729, 2014 www.atmos-chem-phys.net/14/11711/2014/doi:10.5194/acp-14-11711-2014) have studied using a statistical proxy based on Mikkonen et al 2011 (Atmos. Chem. Phys., 11, 11319–11334, doi:10.5194/acp-11-11319-2011, 2011.) This lead to a better agreement in boundary layer with measurements. However, the proxy is a function of radiation and is thus linked to clouds which do not have a significant role on the OH-concentration in the stratosphere.

Since the earlier formulation indicated that there was something problematic with the oxidation of SO2 (which was not our purpose) the text is now rewritten,.:

"One possible explanation to the larger burden and effective radius in the model could be that the amount of erupted sulfur is overestimated in the model compared to the real Pinatubo eruption. Recent global stratospheric aerosol studies indicate a much better agreement with observations if they assume a smaller amount of the volcanic SO2 emission of 5 to 7 Tg S(Dohmse et al. 2014; Sheng et al., 2015). Another possible explanation is that a larger proportion of sulfur was removed from the stratosphere during first months after the eruption due the cross tropopause transport out of stratosphere or the enhanced removal with ash and ice cloud (Dhomse et al 2014), Unfortunately, there is only limited amount of observations after the eruption of Pinatubo which makes comparison between model results and observations difficult. However, our results here are similar to the previous model studies (Niemeier et al 2009, English et al 2012, Dhomse et al 2014, Sheng et al 2015).

The statement that "in July polar vortices are weaker" needs to be corrected. In July there is no polar vortex in the Arctic, solely a solid body (anticyclonic) circulation. The polar vortex in the Arctic (and Antarctic, where of course the seasons are shifted) is only present in the winter/spring period. The transport barrier at the edge of the vortex is indeed most strongly pronounced in winter. Important for the arguments here might also be the seasonal variability of the transport barrier between the subtropics and tropics (there are a number of recent studies on this issue), which should be discussed here.

Text are now modified and argument about subtropical barrier is now added to the text:

"In contrast, in July the atmospheric flow is towards north at the northern high latitudes (Fig. B1) and the sulfur stays in the Arctic. At the same time, the seasonality of subtropical barrier affects how sulfate is transported to the tropics. As figure B1 shows, winds in the northern border of the tropics are towards south only between April and July and sulfur is transported to the tropic only during this time period. There is clearly more sulfate at the northern border of the tropics during these months after the Arctic eruption in January while most of the sulfate is already removed from the atmosphere if volcano was erupted in July. Thus.."

All minor comments below have been fixed if not otherwise said.

throughout the paper: replace 'volcano eruption' by 'volcanic eruption'
p 21839, l 9: aerosol aerosol particles

p 21839, l 25: decades or centuries?

We would like to think that decades. There could be many opinions about this, but if SRM is going to be used for centuries, we would argue that it is used for wrong purposes (as an alternative to GHG reduction)

p 21840, l 1: papers by Robock 2000 'and' Timmreck . . .
p 21841, l 21: a number the number
p 21841, l 22: a number concentration one number concentration
p 21842, l 14: a sea sea
p. 21845, l 14: citation for 8.5 Tg

p. 21850, l 14: quantify 'faster'

'Faster' cannot be easily quantified, since it is so much dependent on aerosol size and atmospheric circulation.

p. 21851, l 4: restarted
p. 21851, l 21: quantify 'quite large'

“ (±0.67 K compared the mean of the ensemble)”-added

p. 21852, l 2: Isn’t ‘cooling’ a radiative effect’ – I think I know what you mean but the point could be made a bit clearer here.

Text is now rewritten as follows:

“Similar to Volc simulation, the global mean temperature is lower compared to the pre-eruption level even radiative forcing has leveled off.”

p 21853, l 3: to low at low
p 21855, l 17: reduction compared to what?
p 21859 l 24: poleward transport of what?

Throughout the paper there are little issues in the text where a "the" is missing or should be replaced by "a". Please correct.

We have done our best to correct this issue; however, none of the authors are native speakers of English. The final text will be polished off by the ACP copy-editing team.

In acknowledgements: Julich Jülich; also Center ‘of’ Climate . . . (l. 7, p. 21864)

Referee #2 comments:

The main conclusion of the paper is that the impacts of a volcanic eruption would be “significantly different depending on whether the eruption occurs during SRM deployment or into a clean background stratosphere” (pg 21857, lines 17-19). In fact, the results could be used to argue the opposite.

In Fig 2, the peak sulfate burden reached after a volcanic eruption during continuous SRM (“SRM Cont”) is identical to the sum of the individual results of SRM alone and an eruption alone. (There are some differences in burden between months 10 and 20, but these seem small compared to the peak burden, and the significance of this difference is impossible to judge from single ensemble members). Similarly, global mean temperature and precipitation responses shown in Fig 4 are consistent (within error bars) for the “Volc” and “SRM Cont” experiments, which implies that the background state has little-to-no impact on the climate response to a volcanic eruption

The discrepancy between the author’s conclusions and those above originates from the definition of what exactly “during SRM deployment” means. The paper puts most of its focus on simulations of a scenario where SRM is employed before the eruption, but suspended upon the occurrence of the eruption. (The authors argue that this the most likely scenario, but one could counterargue that the politics of SRM deployment would be so complicated that it is near impossible to state with any confidence what might be most likely.) Since the difference between the results of the “Volc” and “SRM Cont” simulations are small (as argued above), the conclusions described in the abstract and conclusion section are not due to the existence of SRM before the eruption, but to the sudden suspension of SRM at the time of the eruption. This (as the authors acknowledge within the manuscript) is a trivial result, and very specific to the scenario constructed. Unfortunately, this is not well communicated in the text of the abstract nor the conclusions, and I think many readers could understand that the study finds a significant decrease in the volcanic response under continuous SRM. A readers confusion might be justified, since a comparison of the simulations of volcanic eruptions under background and continuous SRM is the more natural experiment, where only one parameter is being changed between the simulations. The authors’ choice to fo- cus primarily on the SRM scenario with a sudden stop therefore increases the chance for misinterpretation and seems to oversell the role of aerosol size in the radiative and climate impacts of volcanic eruptions, at least for the scenarios explored here.

While we would still argue that suspending SRM following a massive eruption is the most likely scenario (both because of safety and financial considerations), we admit that it is impossible to say for certain whether SRM would be suspended completely, immediately after the eruption or later (if at all). Here we have studied two boundary cases, one where injections are suspended completely immediately after the eruption and another where injections are continued despite the eruption. A “real-life” scenario could be either one of these, or a combination of these two (i.e. SRM is suspended at some point after the eruption or the amount of injected sulfur is decreased). Therefore, the reviewer‘s suggestions on reformulating parts of the abstract and conclusions have been taken into account.

The abstract now reads:

“ -- *According to our simulations the radiative impacts of the eruption and SRM are not additive and the radiative and climate impacts of the eruption depend strongly on whether SRM is continued or suspended after the eruption. In the former case, the peak burden of the additional stratospheric sulfate as well as changes in global mean precipitation are fairly similar regardless of whether the eruption takes place in a SRM or non-SRM world. However, the maximum increase in the global forcing is approximately 30% lower compared to a case when the eruption occurs in an unperturbed atmosphere. In addition, the recovery of the stratospheric sulfur burden and forcing is significantly faster in the concurrent case because the eruption during the SRM leads to a smaller number of larger sulfate particles compared to the eruption in a non-SRM world. On the other hand, if SRM is suspended immediately after the eruption, the peak increase in global forcing is about 40% lower compared to a corresponding eruption into a clean background atmosphere. In addition, the recovery of the stratospheric sulfur burden and forcing is significantly faster in the concurrent case. In this simulation, a volcanic eruption leads to only about 1/3 of the peak global ensemble-mean cooling compared to an eruption under unperturbed atmospheric conditions. Furthermore, the global cooling signal is seen only for the 12 months after the eruption in the former scenario compared to over 40 months in the latter. In terms of global precipitation rate, we obtain a 36% smaller decrease in the first year after the eruption and again a clearly faster recovery in the concurrent eruption and SRM scenario, which is suspended after the eruption. We also found that an explosive eruption could lead to significantly different regional climate responses depending on whether it takes place during geoengineering or into an unperturbed background atmosphere. Our results imply that observations from previous large eruptions, such as Mt*

Pinatubo in 1991, are not directly applicable when estimating the potential consequences of a volcanic eruption during stratospheric geoengineering.“

The relevant parts of the results now read:

“Figure 4a also shows that on average a volcanic eruption during continued SRM (simulation SRM Cont, red line) leads to on average 33% smaller cooling for next three years after the eruption than under unperturbed atmospheric conditions. If SRM is suspended (SRM Volc), the maximum value of the global cooling is only about 1/3 (i.e. less than 0.14 K at maximum for the ensemble mean) compared to an eruption to the non-geoengineered background stratosphere (simulation Volc). This is consistent with the clearly smaller radiative forcings.”

The relevant parts of the conclusions now read:

“According to our simulations, the impacts of a volcanic eruption during SRM depend strongly on whether SRM is continued or halted after the eruption. In the former case, the peak additional forcing is about 30% lower and the global cooling 33% smaller than compared to an eruption taking place in non-SRM world. However, the peak additional burden and changes in global mean precipitation are fairly similar regardless of whether the eruption takes place in a SRM or non-SRM world. On the other hand, if SRM is stopped immediately after the eruption, the peak burden is 24% and forcing 40% lower and reached earlier compared to the case with unperturbed atmosphere. Furthermore, the forcing from the eruption declines significantly faster, implying that if SRM was stopped after the eruption, it would need to be restarted relatively soon (in our scenario within 10 months) after the eruption to maintain the pre-eruption forcing level.”

The paper describes differences in regional precipitation patterns between the different scenarios. The significance of the precipitation anomalies in the three volcanic scenarios is weak outside of the tropics, due likely to the high natural variability and the relatively short runs and few ensemble members. Therefore, the conclusion that precipitation anomalies after an eruption during SRM would be different than during background conditions is not well supported by the results, since it is not shown whether the differences between the scenarios is significant.

We agree and have already explicitly stated the lack of statistical significance both in the text and in the figures (the hatching indicates regions with statistically significant changes). However, we decided to show also the regional precipitation changes, since they are a much discussed aspect of geoengineering. The uncertainty in regional precipitation is not caused by our specific simulation set-ups, but related to natural variability in precipitation and generally models' capability to simulate changes in precipitation. However, the text has now been modified to recognize these uncertainties even more explicitly.

Furthermore, a major caveat is that if SRM is ever employed, it will be under elevated CO2 concentrations, which are not accounted for here. The combination of SRM and CO2 forcing would lead to different total temperature and precipitation anomalies than shown in panels (a) of Figs 5 and 6, therefore the impact of volcanic forcing (e.g., on the meridional temperature gradient) would likely be different in the real world case (with SRM and CO2 forcing) than in these simulations with only SRM.

We agree that SRM without warming from CO2 is an unrealistic scenario. Here we want to study and compare impacts from SRM and/or volcanic eruption in a simplified set-up. However, we have now highlighted the point raised by the reviewer in the text:

"However, it should be noted that here we have studied an unrealistic scenario where SRM is implemented without global warming. If warming from increased greenhouse gases had been included in the scenarios, the temperature gradient could be very different in simulation SRM which could lead to different precipitation patterns. There is also a large natural variability in the precipitation rates and as the precipitation changes after the eruption are relatively small, our results are statistically significant only in a relatively small area (hatching in Fig. 6). "

Appendix A, which validates the model results compared to observations of the Pinatubo eruption, serves a valuable purpose in regards to the paper and is justifiably included as an appendix to sharpen the focus of the main text. If anything, Appendix A would benefit from more material, a comparison of simulated and observed AOD seems to be missing. On the other hand, Appendix B contains results which seem to be outside the scope of the rest of the paper, and only briefly described and explained with little more than speculative reasoning. Either these results should be incorporated into the main results of the paper and more thoroughly explained, or removed from the manuscript.

While a more detailed comparison of the model to observations in Appendix A could be interesting, it is out of the scope of this study. For ECHAM-HAM a more detailed comparison has already made (Niemeier et al 2009, Toohey et al 2011). However this would require changes in mode widths which is used to represent size distribution. After these changes, modelling tropospheric aerosols is not feasible anymore. Here we have used different microphysical aerosol model (M7 -> SALSA) which allows us simulate both stratospheric and tropospheric emissions with basic model setup. Compared to the previous comparisons, using SALSA instead of M7 affect mainly to particle size which is evaluated by comparing effective radius and global sulfate burden (which basically shows lifetime of particle which is related to the particle size). We think that these would be relevant scenarios to study here but the results are not that surprising or significant that those should be included in the main results.

Regarding Appendix B, we feel that it is important to remind the reader that our conclusions are to some extent dependent on the chosen scenario, and that for example different eruption location or season could lead to different results. In the first drafts of this manuscript the appendix material was incorporated within the main text, but several of the co-authors found the main storyline easier to follow once it was moved to an appendix. We have therefore left Appendix B as it was.

All minor comments have been fixed if not otherwise said.

P21838 L10: "decay" might be a better word choice than "recovery"

P21839 L23: "very likely" seems a strong statement given uncertainties in eruption return rates and the term of (hypothetical) SRM. For instance, between Katmai and Pinatubo passed almost 80 years. So it seems one could easily do SRM for 30-50 years and not have a major eruption.

"very likely" changed to "possible"

P21840 L8,11: no 's on Max Planck Institute

P21840 L10: The Niemeier and Stier references don't pertain to HAM-SALSA specifically.

P21841 L10: There is a stratospheric version of HAM. It might be explained why you have not used this version.

We are using sectional microphysical aerosol model SALSA instead of modal model M7. Using a stratospheric model of M7 basically mean using narrower mode width for coarse particles. In SALSA basic configuration is suitable for simulate stratospheric aerosols.

Sec 2.2: It is not clear in the experimental description (esp. for the SALSA simulations) how many ensemble members have been run, and whether the results shown are ensemble means or single ensemble members.

In this section we just want to describe scenarios and these should be included in previous section.

We added to section 2.1.1: "*Only one MAECHAM5-HAM-SALSA simulation has been performed for each of the studied scenarios to obtain the aerosol optical fields for the ESM simulations. Only for Volc we have carried out a five member ensemble to address potential forcing uncertainties (Appendix A).*"

P21845 L14: How well constrained is the 8.5 Tg S for Pinatubo?

This value is based on TOMS/TOVS and MLS satellite observations (Guo et al.,2004b; Read et al., 1993), and is the same as was used in previous studies with ECHAM-HAM (Toohey et al 2011 and Niemeier et al 2009).

P21846 L24: "yr-1" should be removed?**

P21847 L14: The SW forcing seems to oscillate a fair degree, so it might be wrong to call it "steady state"at least, you might clarify that the -6.22 Wm-2 is an average value.**

"Steady state forcing" is changed to *"average global mean forcing"*

P21848 L14: Here we learn that Fig 2 shows a single ensemble member. Why not take the ensemble mean (and show the variability of the ensemble with error bars)?

Since running ECHAM-HAM-SALSA (i.e. explicit aerosol microphysics model within a full atmospheric model) is computationally heavy and since there was not that large a variation in global mean values between single ensemble members, we decided not to run multimember ensembles for all the scenarios.

P21849 L1-5,21-30: The significance of the difference between the "SRM Cont" and the sum of the "Volc" and "SRM" experiments is not convincing, with only single ensemble members shown and no error bars, see major comments.

We now mention in the abstract and conclusions that the differences between these two cases are mostly small.

P21851 L24: Another example of a statement which could be easily misinterpreted, since the SRM scenario used here includes a suspension at the time of the eruption, which is not readily clear from the immediate context.

This is now changed: *"Figure 4a also shows that on average a volcanic eruption during continued SRM (simulation SRM Cont, red line) leads to on average 33% smaller cooling for next three years after the eruption than under unperturbed atmospheric conditions. If SRM is suspended (SRM Volc), the maximum value of the global cooling is only about 1/3 (i.e. less than 0.14 K at maximum for the ensemble mean) compared to an eruption to the non-geoengineered background stratosphere (simulation Volc). This is consistent with the clearly smaller radiative forcings."*

P21853 L13: Driscoll et al., 2012 shows that models don't produce the winter warming pattern.

This is correct, CMIP5 models have problems to reproduce the winter warming. However some of the CMIP5 models produce a warming in winter, but much weaker than observed. This sentence is now rewritten to:

"Winter warming after a volcanic eruption has been seen also in observations (e.g. Robock and Mao 1992, Fischer et al., 2007)), though the current generation of CMIP5 models has problems to reproduce thee NH postvolcanic winter warming pattern (Driscoll et al. 2012) "

P21855 L16: This idea has been around for much longer than since 2013, see e.g., Bala, G., P. B. Duffy, and K. E. Taylor (2008), Impact of geoengineering schemes on the global hydrological cycle., Proc. Natl. Acad. Sci. U. S. A., 105(22), 7664–9, doi:10.1073/pnas.0711648105.

Added

P21856 L21: In the SE Pacific yes, but it's not clear if this opposite response holds for "most of the tropics".

This has been specified to concern Pacific and Atlantic.

P21858 L28: This explanation for the widening of the ITCZ in the simulations seems inconsistent with the understanding of the observed widening of the tropical belt being related to a decrease in the meridional temperature gradient. See Adam, O., T. Schneider, and N. Harnik (2014), Role of Changes in Mean Temperatures versus Temperature Gradients in the Recent Widening of the Hadley Circulation, J. Clim., 27(19), 7450–7461, doi:10.1175/JCLI-D-14-00140.1

Our results are not contradictory to Adam et al. Here the temperature gradient increases in SRM which would lead to the narrowing of the Hadley cell. However making conclusions about ITCZ would require a larger ensemble for further detailed investigations. Based on this, we have now removed the text concerning ITCZ and added discussion about different temperature pattern within the Tropics, which would explain the different precipitation patterns between the scenarios.

Text is now rewritten as follows:

""Similar to the temperature change, our simulations indicate that a tropical volcanic eruption impacts precipitation patterns differently in unperturbed and SRM conditions. In fact, a volcanic eruption during geoengineering (SRM Volc and SRM Cont) leads to an opposite precipitation change pattern than an eruption to the unperturbed atmosphere (Volc) over the

tropic area in Pacific and Atlantic (Fig. 6c and 6d). In these areas, a volcanic eruption during SRM leads to the increase in the evaporation flux at the surface during the first year after the eruption, whereas the evaporation flux decreases if the eruption takes place in unperturbed conditions. This is caused by different tropical temperature responses between the simulations (Fig. 5). Compared to the pre-eruption values, in simulations SRM and Volc, equatorial SST anomalies (latitudes 0 N - 10 N) are relatively colder than the SST anomalies over latitudes 10 N - 20 N. In simulation SRM, the difference in SST anomaly between these areas is -0.02 K and in simulation Volc, it is -0.05 K. On the other hand, in simulations SRM Volc and SRM Conc, equatorial SST anomalies are relatively warmer than those over latitudes 10 N - 20 N. In SRM Volc, the difference in temperature anomaly is 0.13 K and in SRM Cont it is 0.05 K. However, these changes are not significant and a larger ensemble would be necessary for further detailed investigations.“

Referee #3 comments:

Some discussion on the altitude of eruption would be nice. Could the impact in a geoingeneered stratosphere be different when emitting at e.g. 16-18km altitude?

We have added:

*“It should be noted that the impact after concurrent volcanic eruption and SRM may depend also on the altitude at which sulfur is released. Increasing the injection height increases the lifetime of sulfate (Niemeier and Timmreck 2015)***.** *If sulfur from the eruption is released at the same altitude where SRM sulfur resides, it might lead to locally to larger sulfur concentration and therefore to larger particles compared to a case when sulfur from the eruption is released below the SRM sulfate layer. Dependent on the geographical location this volcanic sulfur can still reach the SRM layer e.g in the case of tropical eruption with the ascending branch of the Brewer Dobson circulation. However, this happens on much longer time scales””*

The authors should include a reasoning behind using fixed sea surface temperature, and also a short discussion on the expected impact of a fully coupled ocean.

As has been seen also from the results, there is large variation in the results from MPI-ESM and thus ensemble of several simulations is required. In addition, scenarios by coupled model would require a very long spin up period. Simulations by aerosol-climate model are computational heavy and thus coupling aerosol-climate model with ocean model would require long simulation with computational heavy model which is not possible with limited computational resources. Stratospheric sulfur distribution is not strongly influenced by the ocean and aerosol microphysical simulations without ocean model are justified.

All minor comments below have been fixed if not otherwise said

P21843. L6: Consider referring to Sect. 2.2.

References to scenarios is now added:

"All runs are preceded by a two-year spin-up period followed by a five-year simulation period for the baseline scenarios (defined in section 2.2) and a three-year simulation period for the sensitivity scenarios (Appendix B)."

P21845, L20: "...-SALSA simulations" -> "...-SALSA simulations in the stratosphere".

Modified to: *"and then with MPI-ESM using the stratospheric aerosol fields from MAECHAM5-HAM-SALSA simulations"*

P21846, L3: Remove comma after "study".

P21848, L14-16: Remove parentheses.

P21849, L19: "very fast": To my understanding this means much faster than the responses in question. Suggest rephrase.

"very fast" is replaced by "within less than a year"

P21849, L25-28: Skip parentheses and rewrite the latter part ("and therefore effectively scales" -> "scaling well with SRMcont" ? "corresponding well with SRMcont"?).

This is now rewritten as:

"There is a similar increase in the sulfate burden in the first ten months after the eruption in the Volc and SRM Cont scenarios as is seen by comparing the red and purple lines in Figure 2; here the purple dashed line shows the calculated sum of the effects from separate simulations of Volc and SRM. This scales the Volc simulation to the same start level as SRM Cont. After the first ten months the sulfate burden"

P21850, L3: Lower than what?

"than after the eruption in Volc. "

P21850, L16: How is the growth rate of particles? Is it fast/slow, and have you tested how different growth rates will affect the results?

We haven't tested how different growth rates would affect the results. The growth rate is calculated according to a well-established condensation and coagulation equations, and therefore testing other growth rates would require somehow artificially modifying these equations (or alternatively changing the amount of condensable material, i.e. in this case H_2SO_4 from SO_2 injections, which is out of the scope of this study).

P21851, L4: "be restart" -> "be restarted".

P21852, L1-3: "similar to background conditions": This is an unclear sentence, please rewrite. You are discussing Volc vs SRM Volc?

We have changed to:

"*similar to Volc, ---"*

P21855, L1-5: How large is the changes in longwave radiative forcing?

We have added:

"This in turn leads to an overestimation of the longwave radiative forcing (0.7 W/m^2 for SRM) while the shortwave forcing is less affected (-0.2 W/m^2 for SRM)."

P21855, L12: Suggest moving "lead" to after "eruption".

P21855, L19: "than after" -> "than the impact of" ?

P21856, L16: Less evaporation: Do you mean net evaporation? If not, are there perhaps changes in condensation also?

Here we discuss evaporation fluxes at the surface. This is now added to the text.

P21858, L16-17: Unclear sentence. "SRM case" and "as well as the SRM-only case".

Rewritten: *"Interestingly, the sign of the precipitation change was opposite in SRM Volc and SRM Cont than in the Volc and SRM in large parts of the tropical Pacific."*

P21858, L18: Could any of the changes be due to longwave forcing?

Some of changes might be due the changes in the LW radiation, but here LW radiation have relatively small contribution compared to the changes in SW radiation. .

P21860, L11: "are depended" -> "depend" or "are dependent"

Radiative and climate impacts of a large volcanic eruption during stratospheric sulfur geoengineering

A. Laakso[1], H. Kokkola[1], A.-I. Partanen[2,3], U. Niemeier[4], C. Timmreck[4], K. E. J. Lehtinen[1,5], H. Hakkarainen[6] and H. Korhonen[2]

[1]{Finnish Meteorological Institute, Atmospheric Research Centre of Eastern Finland, Kuopio, Finland}

[2]{Finnish Meteorological Institute, Climate Research, Helsinki, Finland}

[3]{Department of Geography, Planning and Environment, Concordia University, Montreal, Quebec, Canada}

[4]{Max Planck Institute for Meteorology, Hamburg, Germany}

[5]{Department of Applied Physics, University of Eastern Finland, Kuopio campus, Kuopio, Finland}

[6]{A. I. Virtanen Institute for Molecular Sciences, University of Eastern Finland, Kuopio, Finland.}

Correspondence to: A. Laakso (anton.laakso@fmi.fi)

Abstract

Both explosive volcanic eruptions, which emit sulfur dioxide into the stratosphere, and stratospheric geoengineering via sulfur injections can potentially cool the climate by increasing the amount of scattering particles in the atmosphere. Here we employ a global aerosol-climate model and an earth system model to study the radiative and climate impacts of an erupting volcano during solar radiation management (SRM). ~~According to our simulations the radiative impacts of the eruption and SRM are not additive: in the simulated case of concurrent eruption and SRM, the peak increase in global forcing is about 30% lower compared to a corresponding eruption into a clean background atmosphere. In addition, the recovery of the stratospheric sulfur burden and forcing is significantly faster in the concurrent case because the eruption during the SRM would lead to a smaller amount of larger sulfate particles compared to the eruption in non SRM world. For the same reasons and by suspending SRM immediately after~~

~~the eruption (for example because of precautionary or financial reasons), a volcanic eruption would lead to only about 1/3 of the peak global ensemble-mean cooling compared to an eruption under unperturbed atmospheric conditions. Furthermore, the global cooling signal is seen only for the 12 months after the eruption in the former scenario compared to over 40 months in the latter. In terms of global precipitation rate, we obtain a 36% smaller decrease in the first year after the eruption and again a clearly faster recovery in the concurrent eruption and suspended SRM scenario. We also found that an explosive eruption could lead to significantly different regional climate responses depending on whether it takes place during geoengineering or into an unperturbed background atmosphere. Our results imply that observations from previous large eruptions, such as Mt Pinatubo in 1991, are not directly applicable when estimating the potential consequences of a volcanic eruption during stratospheric geoengineering.~~ According to our simulations the radiative impacts of the eruption and SRM are not additive and the radiative and climate impacts of the eruption depend strongly on whether SRM is continued or suspended after the eruption. In the former case, the peak burden of the additional stratospheric sulfate as well as changes in global mean precipitation are fairly similar regardless of whether the eruption takes place in a SRM or non-SRM world. However, the maximum increase in the global forcing is approximately 30% lower compared to a case when the eruption occurs in an unperturbed atmosphere. In addition, the recovery of the stratospheric sulfur burden and forcing is significantly faster in the concurrent case because the eruption during the SRM leads to a smaller number of larger sulfate particles compared to the eruption in a non-SRM world. On the other hand, if SRM is suspended immediately after the eruption, the peak increase in global forcing is about 40% lower compared to a corresponding eruption into a clean background atmosphere. In addition, the recovery of the stratospheric sulfur burden and forcing is significantly faster in the concurrent case. In this simulation, a volcanic eruption leads to only about 1/3 of the peak global ensemble-mean cooling compared to an eruption under unperturbed atmospheric conditions. Furthermore, the global cooling signal is seen only for the 12 months after the eruption in the former scenario compared to over 40 months in the latter. In terms of global precipitation rate, we obtain a 36% smaller decrease in the first year after the eruption and again a clearly faster recovery in the concurrent eruption and SRM scenario, which is suspended after the eruption. We also found that an explosive eruption could lead to significantly different regional climate responses depending on whether it takes place during geoengineering or into an unperturbed background atmosphere. Our results imply that observations from previous large eruptions, such as Mt Pinatubo in 1991, are not directly applicable when estimating the potential consequences of a volcanic eruption during stratospheric geoengineering.

1 Introduction

Solar radiation management (SRM) by injecting sulfur to the stratosphere is one of the most discussed geoengineering methods, because it has been suggested to be affordable and effective and its impacts have been thought to be predictable based on volcanic~~o~~ eruptions (Crutzen, 2006, Rasch *et al*, 2008, Robock *et al* 2009 , McClellan *et al 2012*). Stratospheric sulfur injections could be seen as an analogue of explosive volcanic eruptions, during which large amounts of sulfur dioxide (SO_2) are released into the stratosphere. Once released, SO_2 oxidizes and forms aqueous sulfuric acid particle~~aerosol~~s which can grow to large enough sizes (some hundreds of nanometers) to efficiently reflect incoming solar radiation back to space. In the stratosphere, the lifetime of the sulfate particles is much longer (approximately 1-2 years) than in the troposphere, and the cooling effect from sulfate aerosols may last for several years, as has been observed after large volcanic eruptions, such as Mt. Pinatubo in 1991 (Hansen et al 1992, Robock 2000, Stenchikov et al 2009). Stratospheric SRM would maintain a similar aerosol layer in the stratosphere continuously and could therefore be used (at least in theory) as a means to buy time for the greenhouse gas emission reductions (Keith and MacMartin 2015).

One concern in implementing stratospheric SRM is that an explosive eruption could happen while SRM is being deployed. While it is impossible to predict the timing of such eruptions, large volcanic events are fairly frequent with three eruptions in the 20th century suggested having Volcanic Explosivity Index (VEI) value of 6, indicating substantial stratospheric injections (Santa María in 1902, Novarupta/Katmai in 1912, and Pinatubo in 1991) (Robock, 2000). Thus it is ~~very likelyit~~ possible that a large volcanic eruption could happen during SRM deployment, which would most likely be ongoing for decades. Should this happen, it could lead temporarily to a very strong global cooling effect when sulfate particles from both SRM and the volcanic eruption would reflect solar radiation back to space. While the climate effects of volcanic eruptions into an unperturbed atmosphere have been investigated in many previous studies (see overview papers by Robock, 2000 and~~;~~ Timmreck 2012), they may be different if a volcanic eruption took place during SRM. In the unperturbed atmospheric conditions, the stratosphere is almost clean of particles, while during SRM there would already be a large amount of sulfate in the stratosphere prior to the eruption. Thus, the temporal development of the volcanic aerosol size distribution and related to this the volcanic radiative forcing under SRM conditions may behave very different.

Here we study the effects of a volcanic eruption during SRM by using two Max Planck Institute's models, i.e. the general circulation model (GCM) MAECHAM5 (Giorgetta et al, 2006) coupled to an aerosol microphysical module HAM-SALSA (Bergman et al. 2012, Kokkola et al. 2008~~, Niemeier et al., 2009, Stier et al. 2005~~) and the Max Planck Institute~~'s~~ Earth System Model (MPI-ESM) (Giorgetta et al., 2013). We investigate the simulated characteristics of the stratospheric sulfur burden, radiative forcing, and global and regional climate effects.

2 Methods

2.1 Model descriptions

The simulations were performed in two steps. In the first step, we used the aerosol-climate model MAECHAM5-HAM-SALSA to define global aerosol fields in scenarios with stratospheric sulfur injections and/or a volcanic eruption. In the second step, we prescribe the simulated stratospheric aerosol fields from MAECHAM5-HAM-SALSA to MPI-ESM, similar to Timmreck et al (2010).

2.1.1 Defining aerosol fields with MAECHAM5-HAM-SALSA

For the global aerosol simulation we use MAECHAM5-HAM-SALSA. The atmospheric model MAECHAM5 is a middle atmosphere configuration of ECHAM5, in which the atmosphere is divided into 47 height levels reaching up to ~80 km. MAECHAM5 is integrated with a spectral truncation of 63 (T63), which corresponds approximately to a 1.9° x 1.9° horizontal grid. The simulations were performed with a time step of 600 s.

The aerosol module HAM is coupled interactively to MAECHAM5 and it calculates aerosol emissions and removal, gas and liquid phase chemistry, and radiative properties for the major global aerosol compounds of sulfate, organic carbon, black carbon, sea salt and mineral dust.

In the original ECHAM-HAM (Stier et al., 2005), the aerosol size distribution is described with seven lognormal particle modes with fixed standard deviations and is designed to represent the tropospheric aerosol conditions. Therefore, the width of the coarse mode is optimized for description of sea salt and dust particles, and it does not perform well in special cases like volcanic eruptions or SRM, when a fairly monodisperse coarse mode of sulfate particles can form in the stratosphere (Kokkola et al., 2009). Because of this, we chose to use a sectional aerosol model SALSA (Kokkola et al., 2008), which has been previously implemented to ECHAM-HAM (Bergman et al, 2012) and is used to calculate the microphysical processes of nucleation, condensation, coagulation and hydration. SALSA does not restrict the shape of the size distribution making it possible to simulate both tropospheric and stratospheric aerosols with the same aerosol model.

The default SALSA setup divides the aerosol number and volume size distribution into 10 size sections, which are grouped into three subregions (Fig. 1, left panel, distribution a). In addition, it has 10 extra size sections to describe external mixing of the particles (Fig. 1, left hand panel, distributions b and c). In order to keep the~~a~~ number of tracer variables to the minimum, in the third subregion (coarse particles) only a number concentration in each section is tracked and thus the particle dry size is prescribed. This means that the sulfate mass is not explicitly tracked in this region although it is allowed to change the solubility of the dust particles (distribution c in Fig. 1). In addition, there is no coagulation and condensation growth inside this third subregion, although smaller particles and gas molecules can be depleted due to collisions with particles in subregion 3. In standard tropospheric conditions, this kind of description of the coarse particles is sufficient and it saves computational time and resources. However, when studying large volcanic eruptions or stratospheric sulfur geoengineering, microphysical processing of an aerosol by a large amount of stratospheric sulfur can significantly modify also the size distribution of coarse particles during their long lifetime (Kokkola et al., 2009). With the default setup, this processing cannot be reproduced adequately. In addition, information on the sulfur mass in each size section in the coarse size range is not available in the default setup. Thus we modified the SALSA model to exclude the third subregion and broadened the second subregion to cover also the coarse particle range, as is shown in Figure 1 (right hand panel). This allows a better representation of coarse particles in the stratosphere, but increases simulation time by approximately 30% due to an increased number of the particle composition tracers.

In addition to the sulfur emissions from SRM and from volcanic eruptions (described in Section 2.2), the MAECHAM5-HAM-SALSA simulations include aerosol emissions from anthropogenic sources and biomass burning as given in the AEROCOM database for the year 2000 (Dentener et al 2006). For a sea spray emissions, we use a parameterization combining the wind-speed-dependent source functions by Monahan et al (1986) and Smith and Harrison (1998) (Schulz et al 2004). Dust emissions are calculated online as a function of wind speed and hydrological parameters according to the Tegen et al (2002) scheme. We do not include volcanic ash emissions as it has been shown that ash sediments within a few day after the eruption from the stratosphere and the area affected by the ash cloud is relatively small (Guo et al 2004a). We do not include volcanic ash emissions as it has been shown that ash is deposited relatively fast in the atmosphere and an area of the ash cloud is relatively small (Guo et al 2004a) The effect of fine ash on the distribution of the volcanic cloud in the atmosphere is also relatively small (Niemeier et al 2009). and its effect to the sulfate concentration in the atmosphere is small (Niemeier et al 2009).

The MAECHAM5-HAM-SALSA simulations were carried out with a free running setup without nudging. Thus the dynamical feedback resulting from the additional heating from increased stratospheric sulfate load was taken into account. Global aerosol model studies of the Pinatubo eruption (Timmreck et al 1999; Aquial et al 2013) showed that the dynamic response to local aerosol heating has an important influence on the initial dispersal of the volcanic cloud. Performing non-interactive and interactive Pinatubo simulations these studies revealed that an interactive coupling of the aerosol with the radiation scheme is necessary to adequately describe the observed transport characteristics over the first months after the eruption. Only the interactive model simulations where the volcanic aerosol is seen by the radiation scheme are able to simulate the observed initial southward cross-equatorial transport of the cloud as well as the aerosol lifting to higher altitudes. A further improvement of the interactive simulation is a reduced northward transport and an enhanced meridional transport towards the south, which is consistent with satellite observations. On the other hand, not running the model in the nudged mode means that the online emissions of, e.g., sea salt and mineral dust that are sensitive to wind speed at 10 m height, can differ significantly between the simulations. This can occasionally have fairly strong local effects on the aerosol radiative forcing. However, the global radiative forcing from dust is small compared to the forcing from the volcanic eruption and SRM. The radiative forcing resulting from aerosol loadings was calculated using a double call of radiation (with and without aerosols).

Because MAECHAM5-HAM-SALSA does not be coupled to the ocean model, ~~All~~ the ~~MAECHAM5-HAM-SALSA~~ simulations presented below have been done using fixed sea surface temperatures. All runs are preceded by a two-year spin-up period followed by a five-year simulation period for the baseline scenarios (defined in section 2.2) and a three-year simulation period for the sensitivity scenarios (Appendix B). Only one MAECHAM5-HAM-SALSA simulation has been performed for each of the studied scenarios to obtain the aerosol optical fields for the ESM simulations. Only for Volc we have carried out a five member ensemble to address potential forcing uncertainties (Appendix A).

~~Only one simulation has done for each of the studied scenarios (except Volc is repeated to get five simulation ensemble in Appendinx A).~~

2.1.2 Determining climate effects with MPI-ESM

In the second step, simulations to quantify the global and regional climate effects of concurrent SRM and volcanic eruption are performed with the Earth system model MPI-ESM (Giorgetta et al., 2013). The model is a state-of-the-art coupled three-dimensional atmosphere-ocean-land surface model. It includes the atmospheric component ECHAM6 (Stevens et al., 2013), which is the latest version of the atmospheric model ECHAM and whose earlier version is used in the first step of this study. The atmospheric model is coupled to the Max Planck Institute Ocean Model (MPIOM) (Junglaus et al., 2013). MPI-ESM also includes the land model JSBACH (Reich et al., 2013) and the ocean biochemistry model HAMOCC (Ilyina et al., 2013). ECHAM6 was run with the same resolution as in the first part of this study. We did not include dynamical vegetation and carbon cycle in the simulations.

In MPI-ESM, aerosol fields are prescribed. We used the same tropospheric aerosols fields based on the Kinne et al., (2013) climatology in all scenarios. In the stratosphere, we use precalculated aerosol fields from the different simulations with MAECHAM5-HAM-SALSA. The aerosol radiative properties were calculated based on monthly mean values of the aerosol effective radius and the aerosol optical depth (AOD) at 550 nm. MPI-ESM uses a precalculated look-up table to scale AOD at 550 nm to the other radiation wavelengths based on the effective radius. Here MPI-ESM assumes the size distribution to consist of a single mode, which in most cases differs from the sectional size distribution in MAECHAM5-HAM-SALSA. This can lead to somewhat different radiative forcings between MAECHAM5-HAM-SALSA and MPI-ESM. In our study this has be seen as overestimation of both shortwave and longwave forcing. Overestimation is slightly larger in LW-radiation and thus warming effect of MPI-ESM is overestimated in MPI-ESM compared to the simulations by ECHAM-HAM. Since there is very little zonal variation in the monthly mean stratospheric aerosol fields, the zonal mean aerosol fields from MAECHAM5-HAM-SALSA are used in MPI-ESM.

The atmospheric gas concentrations were fixed to year 2010 level, in accordance with the tropospheric aerosol fields and land use maps. Year 2010 concentrations were also used for methane, CFC and nitrous oxide.

Experiments with a full Earth system model require a long spin-up period as the ocean component needs centuries to stabilize. We resolved this by restarting our 105-year-long spin-ups from previously run Coupled Model Intercomparison Project Phase 5 (CMIP5) simulations ending in year 2005. Since the aerosol and atmospheric gas concentrations in our simulations differed slightly from the CMIP5 runs, the 105 years of spin-up was not enough for the model to reach a full steady state; there was a small warming (0.3 K / 100 yr) also after spin-up period in both *CTRL* and *SRM* simulations (see simulation details in Section 2.2). This temperature change is nevertheless so small that it does not affect our conclusions.

Since the initial state of the climate system can have a significant effect on the climate impacts resulting from forcing, we ran 10-member ensembles of 5-year duration for all baseline scenarios with a volcanic eruption. To do this, we first ran the model for 50 years after the spin-up and saved the climate state after every 5 years. We then continued the simulations from each of these saved climate states for further five years with a volcanic eruption taking place in these specific climate conditions. The obtained results were compared to the corresponding 5-year period in the simulations without a volcanic eruption (which were run continuously for 50 years).

2.2 Model experiments

We simulated altogether 5 baseline scenarios in order to investigate the radiative and climate impacts of concurrent SRM and a volcanic eruption. To better separate the effects of SRM and the eruption, these scenarios included also simulations with only SRM or only a volcanic eruption taking place. The studied scenarios are listed in Table 1, and detailed below. Three additional sensitivity simulations investigating the sensitivity of the results to the geographical location and the seasonal timing of the eruption are presented in Appendix B.

All the simulations with SRM assumed continuous injections of 8 Tg(S)/yr of SO_2 between 30° N and 30° S and 20 km – 25 km in the vertical. The injection strength of 8 Tg/yr was chosen based on previously published SRM studies and for example Niemeier et al (2011) has shown such injection rates to lead to all sky global shortwave radiative forcing of -3.2 to– -4.2 W/m^2 in ECHAM5-HAM. This forcing is roughly comparable (but opposite in sign) to forcing from doubling of CO_2 from preindustrial level. Such a strong SRM forcing could be considered realistic in view of the business-as-usual scenario of the Representative Concentration Pathways (RCP8.5), which estimates that without efforts to constrain the greenhouse gas emissions the total radiative forcing from anthropogenic activities at the end of the 21st century is roughly 8.5 W/m^2 (IPCC, 2013). All the simulations with a volcanic eruption assumed an explosive eruption releasing 8.5 Tg of sulfur to the stratosphere (Niemeier et al 2009, Guo et al 2004b, Read et al., 1993). This corresponds to the magnitude of the Mt. Pinatubo eruption in June 1991. In all of the volcanic eruption scenarios, sulfur was injected to the height of 24 km. The eruption was always initiated on the 1st day of the month at 06:00 UTC and it lasted for 3 hours.

The baseline scenarios summarized in Table 1 and detailed below were simulated first with MAECHAM5-HAM-SALSA, and then with MPI-ESM using the stratospheric aerosol fields from MAECHAM5-HAM-SALSA simulations. On the other hand, the sensitivity simulations in Appendix B were run only with MAECHAM5-HAM-SALSA because of the computational expense of the MPI-ESM code.

The control (*CTRL*) simulation included only standard natural and anthropogenic aerosols with no SRM or explosive eruptions, while the simulation *SRM* included SRM on top of the background aerosol, but no volcanic eruption. All the baseline scenarios which simulated a volcanic eruption assumed a tropical eruption at the site of Mt. Pinatubo (15.14° N, 120.35° E), where a real explosive eruption took place in summer 1991. We simulated a July eruption at this site both in background conditions (simulation *Volc*) and during SRM (simulation *SRM Volc and SRM Cont*). Due to safety and economic considerations, it might be that SRM is suspended at some point after the eruption. When this would happen depends on several factors (decision making process, magnitude/timing volcano). Here we study cases where ~~In the latter run,~~ SRM was suspended immediately after the eruption (*SRM Volc*)~~, as would likely be the case due to safety and economic considerations~~. and~~However,~~ we also simulated a scenario where SRM was continued despite the eruption (*SRM Cont*). The purpose of the latter~~this~~ simulation was also to study~~,~~ how additive the radiative effects of volcanic eruption and solar radiation management are. ~~This simulation also demonstrates what would happen if solar radiation management was not suspended after the eruption for some reason.~~

It should be noted that if the SRM injections are suspended after a volcanic eruption, the injections should be restarted after some time from the eruption to prevent abrupt warming. However, we do not simulate the restart of SRM injections in this study.

3 Results

3.1 Microphysical simulations of volcanic eruption and SRM compared to the measurements and previous studies

A comparison of the *Volc* simulation against observations of the Pinatubo 1991 eruption shows that the model reproduces well the temporal behavior of ~~the global stratospheric sulfur burden and the~~ particle effective radius after a tropical eruption (Figure A1b in Appendix A). ~~Furthermore, the magnitude of the burden is also generally well captured by the model, although~~ T~~t~~he model somewhat overestimates the observations from satellite (HIRS) (Baran and Foot, 1994) during the first 12~~0~~ months after the eruption (Figure A1 in Appendix A).. There are several previous global model studies that where evolution of stratospheric aerosols following Pinatubo eruption has been investigated. Many of these shows similar sulfate burden than in the our study and overestimation of sulfate burden compared to the HIRS data (Niemeier et al 2009, English et al 2012, Dhomse et al 2014, Sheng et al 2015). This comparison between the limited set of the observational data and with other modelling studies gives us confidence that the new MAECHAM5-HAM-SALSA set-up simulates reliable aerosol loads and properties under high stratospheric sulfur conditions.

We first looked at the aerosol burdens and the radiative impacts of a tropical volcanic eruption and SRM separately based on the MAECHAM5-HAM-SALSA runs (simulations *Volc* and *SRM*, respectively). The maximum stratospheric sulfate burden after the volcanic eruption (*Volc*) is 8.31 Tg(S). 75% of the erupted SO_2 is oxidized in two months after the eruption, mostly in the summer hemisphere (NH). However some of the SO_2 is spread to the winter hemisphere (SH) where OH concentration in the first months following the eruption is low due to lower solar radiation. As the OH abundance in the SH increases towards spring, the peak burden in this hemisphere is reached around month 5 (Fig. A2b). As a result, also the global maximum of sulfate burden is reached 5 months after the eruption (Fig. 2a, black solid line). After this, the burden starts to decline rapidly, but remains above the level that was simulated prior to the eruption for approximately 4 years. On the other hand, continuous geoengineering with 8 Tg(S)/yr (*SRM*) leads to the global stratospheric sulfate burden of 7.8 Tg with only little variation in time (Fig. 2a, dashed black line). The total sulfur amount (SO_2 and sulfate) in the stratosphere is 8.8 Tg(S) which indicates the average ~~mean~~ sulfur lifetime (sulfur burden divided by the amount of the injected sulfur) in the stratosphere to be 1.1 years. As previous studies have shown, the lifetime of sulfur is strongly dependent on the injection area and height, and the amount of injected sulfur. Some of the studies have shown a lifetime of clearly less than a year for the comparable magnitude of injected sulfur, when sulfur is injected at a lower height than in our study (Heckendorn et al 2009, Pierce et al 2010, Niemeier et al 2011, English et al 2012), slightly under a year when sulfur is injected at the same height as here (Heckendorn et al 2009, Pierce et al 2010), and over a year when sulfur is injected higher (Niemeier et al 2011). Thus, overall our results are in good agreement with the previous studies.

The maximum clear-sky shortwave (SW) surface forcing in the *Volc* simulation reaches -5.73 W/m^2 (Fig. 2b), which is close to the ~~steady state~~ average global mean forcing of -6.22 W/m^2 in the *SRM* simulation, as could be expected based on the similar maximum and steady state sulfate burdens, respectively (Fig 2a). In the presence of clouds, the change in SW all-sky flux in *SRM* is smaller (-4.22 W/m^2) than in clear-sky conditions. Radiative forcing from the SRM is in agreement with previous studies where the forcing effect has been studied with climate models including an explicit aerosol microphysics description. For example, Niemeier et al (2011) showed all-sky SW radiative forcings from –3.2 W/m^2 to -4.2 W/m^2 for 8 Tg(S)/yr injection, and Laakso et al (2012) a forcing of -1.32 W/m^2 for 3 Tg(S) injection. On the other hand, Heckendorn et al (2009) simulated a clearly smaller radiative forcing of -1.68 W/m^2 for 10 Tg(S) injection.

The shortwave radiative effect (-6.22 W/m^2) from the sulfate particles originating from SRM is concentrated relatively uniformly between 60° N and 60° S (not shown) and has seasonal variation roughly from -5.3 W/m^2 to -7.6 W/m^2. SRM leads also to a 0.73 W/m^2 all-sky longwave radiative forcing which is concentrated more strongly in the tropics than in the midlatitudes and polar regions. In the case of the volcanic eruption (*Volc*), forcing is distributed between 30° N and equator for the first 4 months after the eruption. After that, forcing is concentrated more to the midlatitudes than the low latitudes in both hemispheres. It should be noted, however, that the initial state of the atmosphere and local winds over the eruption area at the time of the eruption can have a large impact on the distribution of sulfur released from a short-duration eruption. This can be seen for example in Figure A2, which illustrates the hemispheric sulfur burdens from 5 different ensemble members of the *Volc* simulation (see Appendix A for details). As an example, in one of the ensemble simulations, burden is concentrated much more in the northern hemisphere (NH) (peak value 6.7 Tg (S)) than in the southern hemisphere (SH) (2.2 Tg (S)). This leads to northern and southern hemispheric clear sky forcings of -4.7 and -1.9 W/m2, respectively. However, in another ensemble member sulfate is distributed more uniformly between the hemispheres (4.8 and 3.7 Tg (S) in the NH and SH, respectively) resulting in clear sky forcing of -3.6 W/m^2 in the north and -2.9 W/m^2 in the south.

(In the analysis above (e.g. Fig. 2), we have used simulation *Volc4* from Appendix A, since it resembles most closely the 5-member ensemble mean in terms how sulfate is distributed between the hemispheres.)

3.2 Burden and radiative effects of concurrent volcanic eruption and SRM – Results of aerosol microphysical simulations

Next we investigated whether the radiative impacts from a volcanic eruption taking place during SRM differs from the sum of volcanic eruption –only and SRM-only scenarios discussed in Section 3.1. In order to do this, we compared the SRM only (*SRM*) and volcanic eruption only (*Volc*) simulations with two scenarios of concurrent eruption and SRM: *SRM Volc* where SRM is suspended immediately after the eruption, and *SRM Cont* where SRM is continued after the eruption. The magnitude, timings and locations of the eruption were assumed the same as in *Volc* simulation.

Figure 2 shows the stratospheric sulfur burden and the global clear sky radiative forcing from the four MAECHAM5-HAM-SALSA runs. It is evident that both the stratospheric sulfate burden and the global shortwave radiative forcing reach a maximum value and recover back to pre-eruption level clearly faster if the volcanic eruption happens during SRM than in stratospheric background conditions, as can be seen by comparing the scenario of volcanic eruption concurrent with SRM (solid blue and red lines) to the sum of eruption-only and SRM-only scenarios (dashed purple~~red~~ line). This is the case especially when SRM is suspended immediately after the eruption (simulation *SRM Volc*). In this case, in our simulation set-up, it takes only 10 months for the stratospheric sulfate burden and the global radiative effect to recover to the state before the volcanic eruption. On the other hand, if the eruption happens in stratospheric background conditions (*Volc*), it takes approximately 40 months before the sulfate burden and the radiative effect return to their pre-eruption values. In addition, the global SW radiative forcing reaches a maximum value two months earlier in *SRM Volc* than in *Volc* (Fig. 2b). In comparison to the value before the eruption, the peak increase in radiative forcing is 40% smaller in *SRM Volc* (-3.4 W/m^2) than in *Volc* (-5.7 W/m^2).

The first, somewhat trivial reason for lower and shorter-lasting radiative forcing in *SRM Volc* is that because SRM is suspended immediately after the eruption, the stratospheric sulfur load will recover from both the volcanic eruption and SRM. If the stratospheric background sulfur level is not upheld by continuous sulfur injections as before the eruption, the sulfur burden will return back to the pre-eruption conditions within less than a year~~very fast~~ after the eruption. However, the different responses to a volcanic eruption during background (*Volc*) and SRM (*SRM Volc*) conditions cannot be explained only by suspended SRM injections. This can be seen in Figure 2a in scenario *SRM Cont* (solid red line) where geoengineering is continued after the volcanic eruption: also in this case the lifetime of sulfate particles is shorter than in *Volc*. There is a similar increase in the sulfate burden in the first ten months after the eruption in the *Volc* and *SRM Cont* scenarios ~~(~~as is seen by comparing the red and purple lines in Figure 2; here the purple dashed line shows the calculated sum of the effects from separate simulations of *Volc* and *SRM*. This scales the *Volc* simulation to the same start level as *SRM Cont*. ~~, and therefore effectively scales the *Volc* simulation to the same start level as *SRM Cont*).~~ ~~There~~A~~a~~fter the first ten months the sulfate burden starts to decrease faster in the *SRM Cont* scenario and is back to the level prior to the eruption after 20 months from the eruption, compared with ~40 months in the *Volc* run. The difference between the two scenarios can be seen even more clearly in the shortwave radiative forcing (Fig. 2b). When the volcano erupts during SRM, the contribution of the eruption to the forcing is lower immediately after the eruption than after the eruption in *Volc*.

The reason for these findings is that the initial stratospheric aerosol load is significantly different when the volcanic eruption occurs during stratospheric sulfur geoengineering than under background conditions. If a volcano erupts concurrently with SRM, sulfur from the eruption does not only form new particles but also condenses onto pre-existing particles. Furthermore, the new small particles that are formed after the eruption coagulate effectively with the existing larger particles from the SRM injections. This means that a situation develops where there are fewer but larger particles compared to a case without SRM. The increased particle size can also be seen in Figure 3 which shows the effective radius in the SRM injection area. These larger particles in *SRM Volc* and *SRM Cont* have higher gravitation settling velocities and sediment faster. Thus, about 30 months after the eruption the effective radius in *SRM Volc* becomes even smaller than in simulation *Volc*, when larger particles have sedimented out of the atmosphere in *SRM Volc*. Figure 2 indicates the impact on the radiative forcing. SW scattering gets less effective with increasing particle size (Pierce et al, 2010) and, although the stratospheric sulfur burden is the same in the first months after the eruption in *SRM Cont* and in the sum of *Volc* and *SRM*, there is a clear difference in the radiative forcing. This indicates that the number-to-mass ratio of particles is smaller in *SRM Cont* than in the calculated sum from *Volc* and *SRM.*

Additional sensitivity simulations with MAECHAM5-SALSA discussed in more detail in Appendix B show that the season when the tropical eruption occurs defines how sulfate from the eruption is distributed between the hemispheres. An eruption in January leads to a larger sulfur burden in the northern hemisphere than an eruption in July (Toohey et al 2011, Aquila et al, 2012). This conclusion holds also if the eruption occurs during geoengineering at least in cases, where SRM is implemented evenly to the both hemispheres. In case of an eruption outside the tropics, the season of the eruption can have a large impact on the magnitudes of both the sulfate burden and the global radiative forcing. Therefore it very likely has an impact also on the regional climates which further defines when and where suspended stratospheric sulfur injections should be restarted. However, due to the computational expense of the fully coupled MPI-ESM, we limit our analysis of the climate impacts below only to the baseline scenarios. It should be noted that the impact after concurrent volcanic eruption and SRM may depend also on the altitude at which sulfur is released. Increasing the injection height increases the lifetime of sulfate (Niemeier and Timmreck 2015). If sulfur from the eruption is released at the same altitude where SRM sulfur resides, it might lead to locally to larger sulfur concentration and therefore to larger particles compared to a case when sulfur from the eruption is released below the SRM sulfate layer. Dependent on the geographical location this volcanic sulfur can still reach the SRM layer e.g in the case of tropical eruption with the ascending branch of the Brewer Dobson circulation. However, this happens on much longer time scales.

3.3 Climate effects from concurrent volcanic eruption and SRM – Results of ESM simulations

In this section we investigate how the radiative forcings simulated for the different scenarios in section 3.2 translate into global and regional climate impacts. For this purpose, we implemented the simulated AOD and effective radius of stratospheric sulfate aerosol from MAECHAM5-HAM-SALSA to MPI-ESM, similar to Timmreck et al (2010).

Figure 4a shows the global mean temperature change compared to the pre-eruption climate. Simulation *Volc* (black line) leads to cooling with an ensemble mean peak value of -0.45 K reached six months after the eruption. On average, this cooling impact declines clearly more slowly than the radiative forcing after the eruption (shown in Fig. 2b): One year after the eruption the radiative forcing was 54% of its peak value, and subsequently 18% and 8% of the peak value two and three years after the eruption. On the other hand, the ensemble mean temperature change is one year after the eruption 84% of the peak value. Subsequently, two and three years after the eruption the temperature change is still 53% and 30% of the peak value. It should be noted, however, that the variation in temperature change is quite large between the 10 climate simulation ensemble members (±0.67 K compared the mean of the ensemble). In fact, in some of the ensemble members the pre-eruption temperature is reached already approximately 15 months after the eruption.

Figure 4a also shows that on average a volcanic eruption during continued SRM (simulation *SRM Cont* ~~*Volc*~~, red~~blue~~ line) leads to on average~~ly~~ 33% smaller cooling for next three years after the eruption than under unperturbed atmospheric conditions. If SRM is suspended (*SRM Volc*), the maximum- value of the global cooling is only about 1/3 ~~of the global cooling~~ (i.e. less than 0.14 K at maximum for the ensemble mean) compared to an eruption to the non-geoengineered background stratosphere (simulation *Volc*). This is consistent with the clearly smaller radiative forcings predicted for the eruption during SRM than in the background atmospheric conditions (Fig. 2b). Similar to *Volc* simulation~~the background conditions~~, the ~~cooling impact~~global mean temperature is lower compared to the pre-eruption level even ~~from the volcanic eruption during SRM outlasts its~~ radiative forcing has leveled off~~effect~~. In SRM Volc scenario t~~T~~he global mean shortwave radiative forcing from the sulfate particles has reached the pre-eruption level after 10 months from the eruption but there would be still some global cooling after 12 months from the eruption. Our simulations indicate that if SRM is suspended but not restarted, there is fast warming compared to the pre-eruption temperature within the first 20 months after the eruption. ~~On the other hand, if SRM is not suspended after the eruption (simulation *SRM Cont*, blue line), additional cooling from the eruption would be clearly stronger and would last for a longer period. However, the cooling would still be slightly weaker and disappear slightly faster compared to simulation *Volc*.~~

Figure 5 depicts the regional surface temperature changes simulated in the different scenarios. Geoengineering alone (*SRM*) would lead to global ensemble mean cooling of -1.35 K compared to the *CTRL* case. As figure 5a) shows, cooling is clearly stronger in the northern hemisphere (-1.65 K) than in the southern hemisphere (-1.05 K). The strongest regional cooling is seen in the northern high latitudes (regional average of -2.2 K north of 50° ~~-~~N). The smallest cooling effect, or even slight warming, is predicted over the southern oceans. These general features are consistent with the GeoMIP multimodel intercomparison when only the impact of SRM (and not of combined SRM and CO_2 increase) is considered: Kravitz et al. (2013a) show a very similar decrease in polar temperature when subtracting temperature change under increased CO_2 from the combined SRM and CO_2 increase results.

For the three volcanic eruption scenarios we concentrate on the regional climate impacts during the first year after the eruption. Figure 5 b) shows the one-year-mean temperature anomaly at the surface after a volcanic eruption into the unperturbed ~~clean~~ background stratosphere in simulation *Volc*. As expected, the cooling impact from the volcanic event over the first year following the eruption is clearly smaller than that from continuously deployed SRM. While there are some similar features in the temperature change patterns between Figures 5a and 5b (such as more cooling in the northern than in the southern hemisphere, and warming in the southern Pacific), clear differences also emerge, especially in NH high and mid latitudes where there is less cooling, and in some regions even warming, after the eruption. During the first year after the eruption, sulfate from the tropical eruption is mainly concentrated at~~to~~ low latitudes where there is also strong solar intensity and thus strong radiative effect from the enhanced stratospheric aerosol layer. During the subsequent years, sulfate transport towards the poles causes stronger cooling also in the high latitudes. The global yearly mean temperature change is -0.34 K for the first year after the eruption then decreasing to a value of -0.30 for the second year from the eruption. However, there is an increased temperature response north of 50° N from the first year mean of -0.30 K to the second year mean of -0.44 K. Even though there is larger cooling at the midlatitudes in the second year after the eruption, we see 0.06 K warming north of 75° N in the second boreal winter (December-February) after the eruption. Winter warming after a volcanic eruption has been seen also in observations (e.g. Robock and Mao 1992, Fischer et al., 2007)), though the current generation of CMIP5 models has problems to reproduce thee NH postvolcanic winter warming pattern (Driscoll et al. 2012). ~~Winter warming after a volcanic eruption has been seen also in observations (Robock and Mao 1992) and a previous intercomparison of climate models (Driscoll et all 2012), thought post-volcanic winter is not well produced by the CMIP5 models. and in observations (Robock and Mao 1992).~~

When the eruption takes place during geoengineering and SRM injections are~~is~~ suspended (*SRM Volc*), the global one-year ensemble mean temperature change is only -0.09 K during the first year after the eruption (Fig. 5c). This small global impact is due to the fact that the anomaly in SW radiation after the volcanic eruption is relatively small in magnitude and only about 10 months in duration when geoengineering is suspended after the eruption (Fig. 2b). However, the regional impacts are much stronger and show distinctly different patterns from those in *Volc* (Fig. 5b). *Volc* scenario leads to 0.30 K cooling north from 50° N in the ensemble mean, while there is small warming of 0.02 K in *SRM Volc* after the first year from eruption. The warming is concentrated over the central areas of Canada, where the ensemble mean temperature increase is more than 1 K, and over North Eurasia, where the temperature increase is more than 0.5 K. It should be noted, however, that in most parts of these regions the warming signal is not statistically significant.

There are also differences in the southern hemispheric temperatures between the different scenarios. While *Volc* scenario leads to small -0.02 K mean cooling south of 50° S in the first year after the eruption, there is a warming of 0.14 K in the *SRM Volc* scenario. In addition, over the Pacific equatorial area *Volc* scenario leads to a cooling of more than -0.5 K while *SRM Volc* scenario leads to a warming of more than 0.5 K. These differences between *Volc* and *SRM Volc* simulations imply that previous observations of regional climate impacts after an explosive eruption, such as Pinatubo in 1991, may not offer a reliable analogue for the impacts after an eruption during SRM. It is important to note, however, that just like there were some variations in the global mean temperature between individual ensemble members, there are also variations in regional changes between the members. Variations are the largest over high latitudes, while most of the individual ensemble members are in good agreement at the low latitudes (hatching in Fig. 5), where the change in temperature is the largest.

The main reason for the differences between *Volc* and *SRM Volc* is that in the latter simulation the volcanic eruption is preceded by SRM injections (providing a baseline stratospheric sulfate load) which are suspended immediately after the eruption. Thus, after the eruption the baseline sulfate load starts decreasing, especially far away from the eruption site, and, therefore, during the first year after the eruption there are regions with a positive radiative forcing compared to the pre-eruption level.

We also find that there could be regional warming in some regions after the volcanic eruption even if the SRM injections were still continued (figure 5d, *SRM Cont*). This warming is concentrated to the high latitudes and areas with relatively little solar shortwave radiation but with large stratospheric particles capable of absorbing outgoing longwave radiation. The warming is strongest in the first post-eruption boreal winter when some areas over Canada, Northeast of Europe and western Russia experience over 0.5 K warming (not shown). Such significant regional warming means that the ensemble mean temperature change north of 50° N during the first post eruption winter is only -0.05 K. In some parts of the Southern Ocean a volcanic eruption could enhance the warming signal caused already by SRM (Fig. 5a).

It is also worth to note that the stratospheric sulfur geoengineering with 8 Tg (S)/yr itself leads only to -1.35 K global temperature change in our simulations. Such weak response is likely at least partly due to the radiation calculations in MPI-ESM, which assume a single modal particle size distribution (see section 2.1.2 for details). Compared to a more flat size distribution simulated by the sectional approach of MAECHAM5-HAM-SALSA, this assumption leads to an overestimation longwave (LW) AOD which is calculated from 550nm AOD. This in turn leads to an overestimation of the longwave radiative forcing (0.7 W/m^2 for *SRM*) while the shortwave forcing is less affected (-0.2 W/m^2 for *SRM*). However this does not affect conclusions of this study.

In addition to the changes in surface temperature, volcanic eruptions will also lead to changes in precipitation. Figure 4b shows the global mean precipitation change after a volcanic eruption in the three scenarios. There is a similar decrease in the precipitation in all volcanic scenarios during the first five months after the eruption. Thereafter there is a similar slow increase in the global mean precipitation in the simulations *Volc* and *SRM Cont* but a clearly faster increase in *SRM Volc*. This faster increase would also ~~lead~~, about one year after the eruption, lead to a higher global ensemble mean precipitation compared to the pre-eruption climate.

The global one year mean precipitation change is 0.036 mm/day, 0.023 mm/day and 0.031 mm/day for *Volc, SRM Volc* and *SRM Cont* respectively for the first year after the eruption. Earlier studies (Bala et al. 2008, Kravitz et al 2013a,b, Niemeier et al 2013) have already shown that geoengineering leads to a reduction in the global precipitation compared the climate without geoengineering. In our *SRM* simulation, we obtain a precipitation reduction of 0.11 mm/day (2.8%), which is clearly larger than the impact after the volcanic eruption.

The stratospheric sulfate affects precipitation via two climate system responses. The first one is the rapid adjustment (fast response) due to atmospheric forcing, such as change in solar irradiance, on a short time scale. The second one is the feedback response (slow response) due to temperature changes (Bony et al 2013, Ferraro et al 2014, Fuglestvedt et al 2014, Kravitz et al 2013,). The signals from both of these responses can be seen in Figure 4b, especially in the simulation *SRM Volc* (blue line). During the first months after the eruption, the precipitation drops relatively rapidly which corresponds well with the rapid change in the radiative forcing (Fig. 2b); at the same time, the temperature change in *SRM Volc* is less steep (Fig. 4a). This implies that in the first months following the eruption, the precipitation change is more affected by the change in the radiation than the change in the temperature. On the other hand, after two years from the eruption there is only small SW radiative effect left from the eruption (and the SRM prior to eruption) but there is still a decrease in the global mean precipitation. During this period, precipitation is predominantly affected by the change in temperature.

Figure 6 shows the regional precipitation changes in each of the studied scenarios. The largest changes after geoengineering (*SRM*) are seen in the tropical convective region where SRM reduces the precipitation rate in large areas by as much as 0.5 mm/day (Fig. 6a). This is in good agreement with previous multi-model studies (Kravitz et al 2013a). In our simulations, an increase of the same magnitude in the precipitation rate is predicted just north of Australia, which has not been seen in previous model intercomparisons (Kravitz et al 2013a).

Although the precipitation patterns in *SRM* and *Volc* are similar in low latitudes, differences are seen especially in NH mid- and high latitudes where *SRM* shows clearly larger reduction in precipitation. The zonal mean value is 0.15mm/day in both 50° north and south latitudes. In these areas, there is clearly less evaporation in the *SRM* scenario which is not seen first year after the volcanic eruption (*Volc*) which would lead to different precipitation patterns.

Similar to the temperature change, our simulations indicate that a tropical volcanic eruption impacts precipitation patterns differently in unperturbed and SRM conditions. In fact, a volcanic eruption during geoengineering (*SRM Volc* and *SRM Cont*) leads to an opposite precipitation change pattern than an eruption to the unperturbed atmosphere (*Volc*) over the tropic area in Pacific and Atlantic (Fig. 6c and 6d). In these areas, a volcanic eruption during SRM leads to the increase in the evaporation flux at the surface during the first year after the eruption, whereas the evaporation flux decreases if the eruption takes place in unperturbed conditions. This is caused by different tropical temperature responses between the simulations (Fig. 5). Compared to the pre-eruption values, in simulations *SRM* and *Volc*, equatorial SST anomalies (latitudes 0 N - 10 N) are relatively colder than the SST anomalies over latitudes 10 N - 20 N. In simulation *SRM*, the difference in SST anomaly between these areas is -0.02 K and in simulation *Volc*, it is -0.05 K. On the other hand, in simulations *SRM Volc* and *SRM Conc*, equatorial SST anomalies are relatively warmer than those over latitudes 10° N - 20° N. In *SRM Volc*, the difference in temperature anomaly is 0.13 K and in *SRM Cont* it is 0.05 K. However, these changes in precipitation are not significant and a larger ensemble would be necessary for further detailed investigations. Similar to the temperature change, our simulations indicate that a tropical volcanic eruption impacts precipitation patterns differently in unperturbed and SRM conditions. In fact, a volcanic eruption during geoengineering (*SRM Volc* and *SRM Cont*) leads to an opposite precipitation change pattern than an eruption to the cleanunperturbed atmosphere (*Volc*) throughout most at of the tropic area in Pacific and Atlantics (Fig. 6c and 6d). In these

~~areas, a volcanic eruption during SRM leads to the increase in the evaporation flux at the surface during the first year after the eruption, whereas the evaporation flux decreases if the eruption takes place in unperturbed conditions. This is caused by different tropical and polar surface temperature responses between the simulations (Fig. 5). The temperature gradient between the polar regions and Tropics increase in the SRM scenario.~~ . ~~This shifts the edge of the Intertropical Convergence Zone (ITCZ) towards the pole. The consequence is less precipitation close to the Equator and an increase between 30 and 40 degree. Under volcanic conditions this temperature gradient decreases, and consequently the the edge of the polar extension of the ITCZ shifts towards the low latitudesdecreases and the Equatorial rain fall increases compared to SRM only. However~~ I~~i~~t should also be noted, that here we have studied an unrealistic scenario where SRM is implemented without global warming. If warming from increased greenhouse gases had~~ve~~ included in the scenarios~~been studied~~, the temperature gradient c~~w~~ould be very~~totally~~ different in simulation *SRM* which c~~w~~ould lead to different precipitation patterns. ~~that as~~ T~~t~~here is also a large natural variability in the precipitation rates and as the precipitation changes after the eruption are relatively small, our results are statistically significant only in a relatively small area (hatching in Fig. 6).

4 Summary and conclusions

We have used an aerosol microphysical model coupled to an atmosphere-only GCM as well as an ESM to estimate the combined effects of stratospheric sulfur geoengineering and a large volcanic eruption. First, MAECHAM5-HAM-SALSA was used to define the stratospheric aerosol fields and optical properties in several volcanic eruption and SRM scenarios. Following the approach introduced in Timmreck et al. (2010) and Niemeier et al. (2013), these parameters were then applied in the Max Planck Institute Earth System Model (MPI-ESM) in order to study their effects on the temperature and precipitation.

According to our simulations, the impacts of a volcanic eruption during SRM depend strongly on whether SRM is continued or halted after the eruption. In the former case, the peak additional forcing is about 30% lower and the global cooling 33% smaller than compared to an eruption taking place in non-SRM world. However, the peak additional burden and changes in global mean precipitation are fairly similar regardless of whether the eruption takes place in a SRM or non-SRM world. On the other hand, if SRM is stopped immediately after the eruption, the peak burden is 24% and forcing 40% lower and reached earlier compared to the case with unperturbed atmosphere. According to our simulations, the magnitude and temporal evolution of stratospheric sulfur burden and the radiative effects resulting from a volcanic eruption would be significantly different depending on whether the eruption occurs during SRM deployment or into a unperturbedclean background stratosphere. We find that the peak burden and forcing are clearly lower and reached earlier if the eruption happens during SRM. Furthermore, the forcing from the eruption declines significantly faster, implying that if SRM was stopped after the eruption, it would need to be restarted relatively soon (in our scenario within 10 months) after the eruption to maintain the pre-eruption forcing level. Even if SRM injections were continued, the peak increase in the global mean radiative forcing after eruption would be 30% lower compared to eruption in normal background conditions.

In line with the burden and forcing results, the simulated global and regional climate impacts were also distinctly different depending on whether the volcano erupts during SRM or in the background stratospheric conditions. In the investigated scenarios, a Pinatubo-type eruption during SRM caused a maximum global ensemble-mean cooling of only 0.14 K (assuming that SRM is paused after the eruption) compared to 0.45 K in the background case. On the other hand, the ensemble-mean decline in the precipitation rate was 36% lower for the first year after the eruption during SRM than for the eruption under unperturbed atmospheric conditions. Both the global mean temperature and the precipitation rate recovered to the pre-eruption level in about one year, compared to approximately 40 months in the background case. If SRM was continued despite the large volcanic eruption, climate cooling was only 67% that it was at normal unperturbed atmospheric conditions for three subsequent years after the eruption.

In terms of the regional climate impacts, we found cooling throughout most of the Tropics regardless of whether the eruption took place during SRM or in the background conditions, but a clear warming signal (up to 1°C) in large parts of the mid and high latitudes in the former scenario. While it should be noted that the regional temperature changes were statistically significant mostly only in the tropics, the declining stratospheric aerosol load compared to the pre-eruption level (as a result of switching off SRM after the eruption) offers a plausible physical mechanism for the simulated warming signal in the mid and high latitudes. On the other hand, the largest regional precipitation responses were seen in the tropics. Interestingly, the sign of the precipitation change was opposite in *SRM Volc* and *SRM Cont* ~~the concurrent eruption and SRM case~~ than in the ~~eruption-only case~~*Volc* and *SRM* ~~(as well as the SRM-only case)~~ in large parts of the tropical Pacific. We attribute this difference to a clearly weaker tropical cooling, or in some areas even a slight warming, in the former scenario leading to an increased evaporation in the first year following the eruption.

Based on both the simulated global and regional responses, we conclude that previous observations of explosive volcanic eruptions in stratospheric background conditions, such as Mt Pinatubo eruption in 1991, are likely not directly applicable to estimating the radiative and climate impacts of an eruption during stratospheric geoengineering. The global mean temperature and precipitation decline from the eruption can be significantly alleviated if the SRM is switched off after the eruption; however, large regional impacts could still be expected during the first year following the eruption.

Appendix A: Evaluation of the model: Pinatubo eruption 1991, comparison between model and measurements

This is the first study where ECHAM5-HAM-SALSA has been used to simulate aerosol processes in the stratosphere. To ensure that the model can be applied for simulation of high aerosol load in the stratosphere, we evaluated the model's ability to reproduce the response of the stratospheric aerosol layer to the Mt. Pinatubo eruption in 1991. We simulated the Pinatubo eruption with MAECHAM5-HAM-SALSA making a 5-member ensemble initiated on the 1st July (see simulation *Volc* in section 2.2 for details). In these simulations, we first used the same two-year spin up for all ensemble members. After the spin up, the model was slightly perturbed by a very small change in a model tuning parameter and then run freely for 6 months, in order to create different atmospheric states for the volcano to erupt into. Only after this was the volcanic eruption triggered in the model. Simulated sulfur burdens and particle effective radii were compared against observations from satellite (HIRS) (Baran and Foot, 1994) and lidar measurements *(Ansmann et al., 1997)*, respectively.

Figure A1 shows that the model results are in general in good agreement with the observations. For example, the model correctly indicates that the oxidation of SO_2 and formation of sulfate particles is very fast right after the eruption. However, the simulated sulfate burden peaks at higher values than the observations after which sulfur burden decreases below observed values approximately one year after the eruption. This has been seen also in previous studies (e.g. English et al 2013 and Niemeier et al 2009). English et al. (2013) suggest that this might be because aerosol heating was not included their model. Our model includes the aerosol heating effect and still underestimates the burden. This might be due the poleward transport at the stratosphere which is overestimated in the model (Niemeier et al 2009).

In all of the ensemble members the effective radius is generally overestimated during months 3-8 after the eruption, although there is also large variation in the measured values (Fig A1b). The simulated maximum value for the effective radius is reached 3-4 months earlier than in observations. After eight months from the eruption results from the all model simulations are good agreement with observations.

~~Higher burden and effective radius in the simulations compared to the measurements indicates an overestimation of SO_2 oxidation in the model.~~

One possible explanation to the larger burden and effective radius in the model could be that the amount of erupted sulfur is overestimated in the model compared to the real Pinatubo eruption. Recent global stratospheric aerosol studies indicate a much better agreement with observations if they assume a smaller amount of the volcanic SO2 emission of 5 to 7 Tg S(Dohmse et al. 2014; Sheng et al., 2015). Another possible explanation is that a larger proportion of sulfur was removed from the stratosphere during first months after the eruption due the cross tropopause transport out of stratosphere or the enhanced removal with ash and ice cloud (Dhomse et al 2014). ~~Overestimation of burden and higher effective radius might be explain by that the estimation of amount of erupted sulfur is larger in our study than what it was in Pinatubo eruption and thus in observation. Also SO_2 might be oxidized t~~~~Too fast which would an oxidation of SO_2 would increase the size of the particles compared to measurements and lead to faster accumulation of particle mass, and thus to stronger sedimentation. Niemeier et al (2009) have suggested that an overestimated mass accumulation in MAECHAM could explain the underestimation of sulfate burden after a year from the eruption.~~ Unfortunately, ~~However~~ there is only limited amount of observations after the eruption of Pinatubo which makes comparison between model results and observations difficult. However, o~~O~~ur results here are similar to does not differ significantly from the previous model studies (Niemeier et al 2009, English et al 2012, Dhomse et al 2014, Sheng et al 2015).

There is some variation in the predicted peak burden and effective radii between the five members of the ensemble simulation (Fig. A1). This indicates that the results are dependentd on the local stratospheric conditions at the time of the eruption. Depending on meridional wind patterns during and after the eruption, the released sulfur can be distributed in very different ways between the hemispheres. This can be seen in Figure A2 which shows the sulfate burdens after the eruption separately in the northern and southern hemispheres. As the figure shows, in simulation *Volc1* over 70% of the sulfate from the eruption is distributed to the northern hemisphere, whereas in *Volc5* simulation it is distributed quite evenly to both hemispheres. These very different spatial distributions of sulfate lead to the aerosol optical depth (AOD) fields illustrated in Figure A3. The AOD in the northern hemisphere is clearly higher in the *Volc1* simulation (panel a) than in the *Volc5* simulation (panel b) for about 18 months after the eruption, whereas the opposite is true for the southern hemisphere for approximately the first two years following the eruption. These results highlight that when investigating the climate effects of a volcanic eruption during SRM, an ensemble approach is necessary.

Appendix B: Sensitivity simulations: Location and season of the eruption

Description of sensitivity runs

We also performed a set of sensitivity simulations to investigate how the season and location of the volcanic eruption during SRM impacts the global sulfate burden and radiative forcing. The baseline scenario *SRM Volc* was compared with three new simulations summarized in Table B1 and detailed below. These sensitivity runs were performed only using MAECHAM5-HAM-SALSA due to the high computational cost of the full ESM, and are therefore limited to analysis of sulfur burdens and radiative forcings.

In the baseline simulations the eruption took place in the tropics. Because the predominant meridional transport in the stratosphere is from the tropics towards the poles, sulfur released in the tropics is expected to spread throughout most of the stratosphere. On the other hand, sulfate released in the mid or high latitudes will spread less effectively to the lower latitudes, and an eruption at mid or high latitudes will therefore lead to more local effects in only one hemisphere. Therefore we conducted a sensitivity run simulating a July eruption during SRM at Mt. Katmai (Novarupta) (58.2° N, 155° W) where a real eruption took place near the northern arctic area in year 1912 (simulation *SRM Arc July*).

The local stratospheric circulation patterns over the eruption site will also affect how the released sulfur will be transported. Furthermore, stratospheric circulation patterns are depended on the season and thus sulfur transport and subsequent climate effects can be dependent on the time of the year when the eruption occurs. For example, the meridional transport toward the poles is much stronger in the winter than in the summer hemisphere (Fig B1). For this reason, we repeated both the tropical and the Arctic volcanic eruption scenarios assuming that the eruption took place in January instead of July (*SRM Volc Jan* and *SRM Arc Jan*, respectively).

Results from sensitivity simulations

Figure B2 shows that the season of the tropical eruption does not significantly affect the stratospheric sulfate burden or the global mean clear-sky radiative forcing (simulations *SRM Volc* and *SRM Volc Jan*). The difference in peak burden values between the simulations with January and July eruptions is under 1% (0.11 Tg (S)) and in peak clear-sky forcing about 1%. Although the timing of the eruption does not have a large impact on the global mean values, there is some asymmetry between the hemispheres as peak value of additional sulfate from the eruption is 54% larger after the tropical NH eruption in July (boreal summer) than in January (boreal winter) (not shown). This is because the predominant meridional wind direction is towards south in July and towards north in January (Fig. B1). Our results are consistent with previous studies (Toohey et al 2011, Aquila et al, 2012) who showed that a Pinatubo type tropical eruption in April would lead to an even increase in AOD in both hemispheres, while a volcanic eruption during other seasons will lead to more asymmetric hemispheric forcings. We show that these results hold also if the eruption takes place during SRM.

On the other hand, if the eruption takes place in the Arctic, the season of the eruption becomes important. Figure B2a shows that a summertime Arctic eruption (*SRM Arc July*) leads to similar global stratospheric peak sulfate burden as the tropical eruptions (*SRM Volc Jan* and *SRM Volc*), although the burden declines much faster after the Arctic eruption. However, an Arctic eruption in January (*SRM Arc Jan*) leads to a global stratospheric sulfate burden peak value that is only ~82% of the July eruption value. The peak value is also reached two months later in the January eruption. Regarding the global forcing (Fig. B2b), an Arctic winter-time eruption (*SRM Arc Jan*) leads to a very similar peak forcing than the tropical eruptions, while the additional peak forcing (compared to the pre-eruption level) is 38% lower if the Arctic eruption takes place in July.

It is interesting to note that in the case of the Arctic volcano, a July eruption leads to a clearly higher stratospheric sulfate peak burden than the January eruption, but the opposite is true for global peak forcing (Fig. B2). A major reason for this is the strong seasonal variation in available solar radiation and subsequently hydroxyl radical (OH) concentration in the high latitudes. OH is the main oxidant that converts SO_2 to sulfuric acid (H_2SO_4). Due to the rising OH concentrations in the Arctic spring, the peak in sulfur burden in the January eruption is reached during the Arctic summer when there is highest amount of sunlight available to be reflected back to space. However, when the eruption takes place in July, the peak burden is reached already in October due to high OH concentrations, and thus much faster compared to the winter-time eruption. However, when the peak value is reached, the intensity of solar radiation has already dramatically decreased, and thus the peak radiative forcing from the eruption remains small. The fast conversion of SO_2 to sulfate also leads to larger particles than after the winter eruption and consequently to faster sedimentation and shorter lifetime (Fig. B2a).

Another main factor that has impact on the climate effects of an Arctic eruption is the stratospheric circulation. Concurrent circulation patterns can influence the sulfate lifetime and radiative effects. As Figure B1 shows, there is a strong seasonal cycle in the Arctic meridional winds. If an Arctic volcano erupts in January, strong zonal polar vortex winds block poleward transport of released sulfur and it can spread towards midlatitudes. In contrast, in July the atmospheric flow is towards north at the northern high latitudes (Fig. B1) ~~tpolar vortices are weaker~~ and the sulfur~~ate~~ stays in the Arctic. At the same time s~~S~~easonality of subtropical barrier affects how sulfate is transported to the tropics. As figure B1 shows, winds in the northern border of the tropics a~~rea~~ are towards south only between April and July and sulfur is transported to the tropic only during this time period.~~,~~ There is clearly more sulfate at the northern border of the tropics during these months~~these area~~ after the Arctic eruption in January while most of the sulfate is already removed from the atmosphere if volcano ~~was~~ erupted in July. Thus a~~A~~fter 6 months of the Arctic eruption, stratospheric sulfur burden in the tropics between 30° N and 30° S is 3.1 Tg (S) for a July eruption but 4.2 Tg (S) for a January eruption. Since the tropics have much more solar radiation for the sulfate particles to scatter than the higher latitudes, part of the stronger radiative forcing in the *SRM Arc Jan* simulation compared to *SRM Arc July* (Fig. B2b) arises from this difference in transport to the tropics. Furthermore, since the lifetime of sulfur is longer in the low than in the high latitudes, this leads to a longer average sulfur lifetime in the *SRM Arc Jan* simulation (Fig. B2a).

Acknowledgements

This work was supported by the Academy of Finland's Research Programme on Climate Change (FICCA) (project 140867), Academy of Finland's Center of Excellence Program (decision 272041), Maj and Tor Nessling foundation (grant 2012116), and Academy of Finland's Academy Research Fellow position (decision 250348). The authors wish to thank T Bergman and S Rast for technical assistance with the models, A Karpecho for helpful discussions related to stratospheric dynamics and T. Kühn for discussions related to using coupled models and A. Baran for comments concerning about HIRS data. The ECHAM–HAMMOZ model is developed by a consortium composed of ETHZ, Max Planck Institut für Meteorologie, Forschungszentrum Jü~~u~~lich, University of Oxford and the Finnish Meteorological Institute and managed by the Center of~~r~~ Climate Systems Modeling (C2SM) at ETHZ.

References

Ansmann, A., Mattis, I., Wandinger, U., Wagner, F., Reichardt, J., and Deshler, T.: Evolution of the pinatubo aerosol: raman lidar observations of particle optical depth, effective radius, mass, and surface area over central europe at 53.4_ N, J. Atmos. Sci., 54, 2630–2641, doi:10.1175/1520-0469(1997)054<2630:EOTPAR>2.0.CO;2, 1997.

Aquila, V., Oman, L. S., Stolarski, R. S., Colarco, P. R. and Newman, P. A., Dispersion of the volcanic sulfate cloud from a Mount Pinatubo–like eruption, J. Geophys. Res. , 117, D06216, doi:10.1029/2011JD016968, 2012.

~~Bergman T., Kerminen V.-M., Korhonen H., Lehtinen K. E. J., Makkonen R., Arola A., Mielonen T., Romakkaniemi S., Kulmala M. and Kokkola H., Geosci. Model. Dev., 5, 845 – 868, 2012.~~

Bala, G., P. B. Duffy, and K. E. Taylor (2008), Impact of geoengineering schemes on the global hydrological cycle., Proc. Natl. Acad. Sci. U. S. A., 105(22), 7664–9, doi:10.1073/pnas.0711648105

Baran, A. J. and Foot, J. S.: New application of the operational sounder HIRS in determining a climatology of sulphuric acid aerosol from the Pinatubo eruption, J. Geophys. Res. Atmos., 99, 25673–25679, 1994.

Bergman T., Kerminen V.-M., Korhonen H., Lehtinen K. E. J., Makkonen R., Arola A., Mielonen T., Romakkaniemi S., Kulmala M. and Kokkola H., Geosci. Model. Dev., 5, 845 – 868, 2012.

Bony, S., G. Bellon, G., D. Klocke, D., S. Sherwood, S., S. Fermepin, S. and S. Denvil, S., Robust direct effect of carbon dioxide on tropical circulation and regional precipitation, Nat. Geosci., 6, 447-451, 2013.

Crutzen, P. J.: Albedo enhancement by stratospheric sulphur injections: A contribution to resolve a policy dilemma?, Climatic Change, 77, 211–219, 2006.

Dentener, F., Kinne, S., Bond, T., Boucher, O., Cofala, J., Generoso, S., Ginoux, P., Gong, S., Hoelzemann, J. J., Ito, A., Marelli, L., Penner, J. E., Putaud, J.-P., Textor, C., Schulz, M., van der Werf, G. R., and Wilson, J.: Emissions of primary aerosol and precursor gases in the years 2000 and 1750 prescribed data-sets for AeroCom, Atmos. Chem. Phys., 6, 4321-4344, doi:10.5194/acp-6-4321-2006, 2006.

Driscoll, S., Bozzo, A., Gray, L. J., Robock, A. and Stenchikov, G., Coupled Model Intercomparison Project 5 (CMIP5) simulations of climate following volcanic eruptions, J. Geophys. Res., 117, D17105, doi:10.1029/2012JD017607, 2012.

Dhomse, S. S., Emmerson, K. M., Mann, G. W., Bellouin, N., Carslaw, K. S., Chipperfield, M. P., Hommel, R., Abraham, N. L., Telford, P., Braesicke, P., Dalvi, M., Johnson, C. E., O'Connor, F., Morgenstern, O., Pyle, J. A., Deshler, T., Zawodny, J. M., and Thomason, L. W.: Aerosol microphysics simulations of the Mt.~Pinatubo eruption with the UM-UKCA composition-climate model, Atmos. Chem. Phys., 14, 11221-11246, doi:10.5194/acp-14-11221-2014, 2014.

English, J. M., Toon, O. B. and, Mills M., J., Microphysical simulations of sulfur burdens from stratospheric sulfur geoengineering. Atmos. Chem. Phys., 12, 4775 - 4792, doi:10.5194/acp-12-4775-2012, 2012.

English, J. M., O. B. Toon, O. J. and M. J. Mills, M. J., Microphysical simulations of large volcanic eruptions: Pinatubo and Toba, J. Geophys. Res. Atmos., 118, 1880–1895, doi:10.1002/jgrd.50196, 2013.

Ferraro, A. J., E. J. Highwood, E. J. and A. J. Charlton-Perez, A. J., Weakened tropical circulation and reduced precipitation in response to geoengineering, Environ. Res. Lett., 9(1), 014001, doi:10.1088/1748-9326/9/1/014001, 2014.

-Fischer, E, Luterbacher, J, Zorita, E, Tett, S.FB, Casty, C, ,Wanner, European climate response to tropical volcanic eruptions over the last half millennium. Geophys. Res. Lett., 34, doi:10.1029/2006 GL027992, 2007.

Fuglestvedt, J.an S. , Bjørn H. Samset, B. J. and Keith P. Shine, K. P.: Counteracting the climate effects of volcanic eruptions using short-lived greenhouse gases, Geophys. Res. Lett., 41,, 8627 - 8635, doi:10.1002/ 2014GL061886, 2014.

Giorgetta, M. A., Manzini, E., Roeckner, E., Esch, M., & Bengtsson, L.. Climatology and forcing of the quasi-biennial oscillation in the MAECHAM5 model. J. Climate, 19(16), 3882-3901, 2006.

Giorgetta, M., M., Jungclaus, J., Reick, C. H., Legutke, S., Bader, J., Böttinger, M., Brovkin, V.,Crueger, T., Esch, M., Fieg, K., Glushak, K., Gayler, V., Haak, H., Hollweg, H.-D., Ilyina, T.,Kinne, S., Kornblueh, L., Matei, D., Mauritsen, T., Mikolajewicz, U., Mueller, W., Notz, D., F., Raddatz, T., Rast, S., Redler, R., Roeckner, E., Schmidt, H., Schnur, R., Segschneider, J., Six, K. D., Stockhause, M., Timmreck, C., Wegner, J., Widmann, H., Wieners, K.-H., Claussen, M., Marotzke, J., and Stevens, B.:et al., Climate and carbon cycle changes from 1850 to 2100 in MPI-ESM simulations for the coupled model intercomparison project phase 5, J. Adv. Model. Earth Syst., 5, 572–597, doi:10.1002/jame.20038, 2013.

Guo, S., Rose, W. I., Bluth, G. J. S., and Watson, I. M.: Particles in the great Pinatubo volcanic cloud of June 1991: The role of ice, Geochem,istry, Geophys.sics, Geosyst.ems, 5, Q05003, doi:10.1029/2003GC000655, 2004a.

Guo, S., G. J. S. Bluth, W. I. Rose, I. M. Watson, and A. J. Prata, Re-evaluation of SO2 release of the 15 June 1991 Pinatubo eruption using ultraviolet and infrared satellite sensors, Geochem. Geophys. Geosyst. , 5 , Q04001, doi:10.1029/ 2003GC000654, 2004b.

Hansen, J., A. Lacis, A., R. Ruedy, R. and M. Sato, M., Potential climate impact of Mount-Pinatubo eruption, Geophys. Res. Lett., 19(2), 215–218, doi:10.1029/91GL02788, 1992.

Heckendorn, P., Weisenstein, D., Fueglistaler, S., Luo, B. P., Rozanov, E., Schraner, M., Thomason, L. W. and Peter, T.. The impact of geoengineering aerosols on stratospheric temperature and ozone, Environ. Res. Lett. 4, 045108, doi: 10.1088/1748-9326/4/4/045108. 2009.

Ilyina, T., Six, K. D., Segschneider, J., Maier-Reimer, E., Li, H., and& Nunez-Riboni, I.. Global ocean biogeochemistry model HAMOCC: Model architecture and performance as component of the MPI-Earth System Model in different CMIP5 experimental realizations.J. Adv. Model. Earth Syst. , 5, 287-315. doi:10.1029/2012MS000178, 2013.

IPCC, 2013: Climate Change 2013: The Physical Science Basis. Contribution of Working Group I to the Fifth Assessment Report of the Intergovernmental Panel on Climate Change [Stocker, T.F., D. Qin, G.-K. Plattner, M. Tignor, S.K. Allen, J. Boschung, A. Nauels, Y. Xia, V. Bex and P.M. Midgley (eds.)]. Cambridge University Press, Cambridge, United Kingdom and New York, NY, USA, 1535 pp, doi:10.1017/CBO9781107415324, 2013.

Jungclaus, J. H., Fischer, N., Haak, H., Lohmann, K., Marotzke, J., Matei, D., Mikolajewicz, U., Notz, D., & von Storch, J.-S.. Characteristics of the ocean simulations in MPIOM, the ocean component of the MPI Earth System Model. J. Adv. Model. Earth Syst. , 5, 422-446. doi:10.1002/jame.20023, 2013.

Keith, D. W. and MacMartin, D. G.. A temporary, moderate and responsive scenario for solar geoengineering. Nature Clim. Change, 5, 201-206, DOI: 10.1038/NCLIMATE2493, 2015.

Kinne, S., D. O'Donnell, D., P. Stier, P., S. Kloster, S., K. Zhang, K., H. Schmidt, H., S. Rast, S., M. Giorgetta, M., T. F. Eck, T.F and B. Stevens, B., MAC-v1: A new global aerosol climatology for climate studies, J. Adv. Model. Earth Syst., 5, 704–740, doi:10.1002/jame.20035, 2013.

Kokkola, H., Korhonen, H., Lehtinen, K. E. J., Makkonen, R., Asmi, A., Järvenoja, S., Anttila, T., Partanen, A.-I., Kulmala, M., Järvinen, H., Laaksonen, A., and Kerminen, V.-M.: SALSA – a Sectional Aerosol module for Large Scale Applications, Atmos. Chem. Phys., 8, 2469-2483, doi:10.5194/acp-8-2469-2008, 2008.

Kokkola, H., Hommel, R., Kazil, J., Niemeier, U., Partanen, A.-I., Feichter, J., and Timmreck, C.: Aerosol microphysics modules in the framework of the ECHAM5 climate model – intercomparison under stratospheric conditions, Geosci. Model Dev., 2, 97–112, http://www.geosci-model-dev.net/2/97/2009/, 2009.

Kravitz, B., Caldeira, K., Boucher, O., Robock, A., Rasch, P. J., Alterskjær, K., Karam, D., B., Cole, J. N. S., Curry, C. L., Haywood, J. M., Irvine, P. J., Ji, D., Jones, A.,Kristjánsson, J. E., Lunt, D. J., Moore, J. C., Niemeier, U., Schmidt, H., Schulz, M., Singh, B., Tilmes, S., Watanabe, S., Yang, S., and Yoon, J.-H.:~~et al.~~, Climate model response from the Geoengineering Model Intercomparison Project (GeoMIP), J. Geophys. Res. Atmos., 118, 8320–8332, doi:10.1002/jgrd.50646, 2013a.

Kravitz, B.~~, et al.~~., Rasch, P. J., Forster, P. M., Andrews, T., Cole, J. N. S., Irvine, P. J., Ji, D., Kristjánsson,J. E., Moore, J. C., Muri, H., Niemeier, U., Robock, A., Singh, B., Tilmes, S., Watanabe, S., and Yoon, J.-H.: , An energetic perspective on hydrological cycle changes in the

Geoengineering Model Intercomparison Project, J. Geophys. Res. Atmos., 118, 13,087–13,102, doi: 10.1002/2013JD020502, 2013b.

Laakso, A., Partanen, A.-I., Kokkola, H., Laaksonen, A., Lehtinen, K. E. J., and Korhonen, H.: Stratospheric passenger flights are likely an ine_cient geoengineering strategy, Environ. Res. Lett., 7, 034021, doi:10.1088/1748-9326/7/3/034021, 2012. Laakso, A., Partanen, A. I., Kokkola, H., Laaksonen, A., Lehtinen, K. E. J., Korhonen, H., Stratospheric passenger flights are likely an inefficient geoengineering strategy Eviron. Res. Lett. 7 034021, 2012.

McClellan, J., Keith, D. W., and Apt, J.: Cost analysis of stratospheric albedo modification delivery systems, Environ. Res. Lett.,7, 034019, doi:10.1088/1748-9326/7/3/034019, 2012.

Monahan, E., Spiel, D. and Davidson, K., Oceanic whitecaps and their role in air-sea exchange pp. 167-174 (D. Reidel, Norwell, Mass.), 1987.

Niemeier, U., Timmreck, C., Graf, H.-F., Kinne, S., Rast, S. and Self, S., Initial fate of fine ash and sulfur from large volcanic eruptions , Atmos. Chem. Phys., 9, 9043-9057, 2009.

Niemeier, U., Schmidt, H. and Timmreck, C., The dependency of geoengineered sulfate aerosol on the emission strategy,Atmos. Sci. Let. 12, 189-194, 2011.

Niemeier, U., H. Schmidt, H.,K. Alterskjær, K. and J. E. Kristjánsson, J.E.,: Solar irradiance reduction via climate engineering: Impact of different techniques on the energy balance and the hydrological cycle, J. Geophys. Res., 118, 12195–12206, 2013.

Niemeier, U. and Timmreck, C.: What is the limit of climate engineering by stratospheric injection of SO_2?, Atmos. Chem. Phys., 15, 9129-9141, doi:10.5194/acp-15-9129-2015, 2015.

Pierce, J. R., Weisenstein, D., Heckendorn, P., Peter, T. and Keith D. W., Efficient formation of stratospheric aerosol for climate engineering by emission of condensible vapor from aircraft, Geophys. Res. Lett. 37 L18805, doi:10.1029/2010GL043975, 2010.

Rasch, P. J., Tilmes, S., Turco, R. P., Robock, A., Oman, Chen C-C, Georgiy L Stenchikov, G. L., Garcia, R., R,, . An overview of geoengineering of climate using stratospheric sulphate aerosols, Phil. Trans. R. Soc. APhilosophical transactions. Series A, Mathematical, physical, and engineering sciences 366, 4007-4037, 2008.

Read, W. G., Froidevaux, L., and Waters, J. W.: Microwave limb sounder measurements of stratospheric SO2 from the Mt. Pinatubo volcano, Geophys. Res. Lett., 20, 1299–1302, 1993.

Reick, C., T. Raddatz, TV., Brovkin, V. and V. Gayler, V., The representation of natural and anthropogenic land cover change in MPI-ESM, J. Adv. Model. Earth Syst., 5, 459-482, doi:10.1002/jame.20022, 2013.

Robock, A. and Mao, J. Winter warming from large volcanic eruptions, Geophys. Res. Lett. 19, 24, 2405-2408, 1992.

Robock, A., Volcanic eruptions and climate, Rev. Geophys., 38(2), 191–219, doi:10.1029/1998RG000054, 2000.

Robock, A., A. Marquardt, AB., Kravitz, B. and G. Stenchikov, G. (2009), Benefits, risks, and costs of stratospheric geoengineering, Geophys. Res. Lett., 36, L19703, doi:10.1029/2009GL039209, 2009.

Schulz, M., de Leeuw, G. and Balkanski, Y., Sea-salt aerosol source functions and emissions, in Emission of Atmospheric Trace Compounds 333-359 Kluwer Acad., Norwell, Mass, 2004.

Sheng, J.-X., Weisenstein, D. K., Luo, B.-P., Rozanov, E., Arfeuille, F., and Peter, T.: A perturbed parameter model ensemble to investigate 1991 Mt Pinatubo's initial sulfur mass emission, Atmos. Chem. Phys. Discuss., 15, 4601-4625, doi:10.5194/acpd-15-4601-2015, 2015.

Smith, M. and Harrison, N., The sea spray generation function. J. Aerosol Sci.. 29, 189-190, 1998.

Stenchikov, G., Delworth, T.L., Ramaswamy, V., Stouffer, R.J., Wittenberg, A. and Zeng, F., Volcanic signals in oceans, J. Geophys. Res., 114, D16104, doi:10.1029/2008JD011673, 2009.

~~Stevens, B., et al., The atmospheric component of the MPI-M Earth System Model: ECHAM6, J. Adv. Model. Earth Syst., 5, 1–27, doi:10.1002/jame.20015., 2013.~~Stevens, B., Giorgetta, M., Esch, M., Mauritsen, T., Crueger, T., Rast, S., Salzmann, M., Schmidt, H., Bader, J., Block, K., Brokopf, R., Fast, I., Kinne, S., Kornblueh, L., Lohmann, U.,Pincus, R., Reichler, T., and Roeckner, E.: The atmospheric component of the MPI-M Earth System Model: ECHAM6, J. Adv. Model. Earth Syst., 5, 1–27, doi:10.1002/jame.20015, 2013.

Stier P. et al. The aerosol-climate model ECHAM5-HAM, Atmos. Chem. Phys. 5, 1125-1156, 2005.

~~Tegen I.~~Tegen, I., Harrison, S. P., Kohfeld, K., Prentice, I. C., Coe, M., and Heimann, M.: ~~et al~~, Impact of vegetation and preferential source areas on global dust aerosol: Results from a model study J. Geophys. Res. 107, ~~4576~~, doi:10.1029/2001JD000963, 2002.

Timmreck, C., H.-F. Graf and I. Kirchner, A one and a half year interactive simulation of Mt. Pinatubo aerosol, J. Geophys. Res.,104, 9337-9360, 1999.

Timmreck, C.: Modeling the climatic e_ects of volcanic eruptions, Wiley Interdisciplinary Reviews: Climate Change, 3, 545–564, doi:10.1002/wcc.192, 2012.

Timmreck, C., H.-F. Graf, H.-F. , S. J. Lorenz, S. J., U. Niemeier, U., D. Zanchettin, D., Matei, D, J. H. Jungclaus, J. H. and T.J. Crowley T.J, (2010), Aerosol size confines climate response to volcanic super-eruptions (2010), Geophys. Res. Lett. 37, L24705, doi:10.1029/2010GL045464,. 2010.

~~Timmreck C., (2012) Modeling the climatic effects of volcanic eruptions, invited review paper Wiley Interdisciplinary Reviews: Climate Change doi: 10.1002/wcc.192, 2012.~~

Toohey, M., Krüger, K., Niemeier, U., and Timmreck, C.: The influence of eruption season on the global aerosol evolution and radiative impact of tropical volcanic eruptions, Atmos. Chem. Phys., 11, 12351-12367, doi:10.5194/acp-11-12351-2011, 2011.

Table 1. Studied sulfur injection and volcanic eruption scenarios.

Scenario	**Description**
CTRL	Control simulation with no SRM or explosive eruptions
SRM	Injections of 8 Tg(S)/yr of SO_2 between latitudes 30° N and 30° S between 20 km – 25 km altitude
Volc	Volcanic eruption at the site of Mt. Pinatubo (15.14° N, 120.35° E) on the first of July. 8.5 Tg of sulfur (as SO_2) injected at 24 km
SRM Volc	Volcanic eruption during SRM. SRM suspended immediately after the eruption
SRM Cont	Volcanic eruption during SRM. SRM still continued after the eruption

Table B1. Sensitivity scenarios run only with MAECHAM5-HAM-SALSA. Here *Jan* refers to a volcanic eruption in January and *Arc* to an Arctic eruption at the site of Katmai.

Scenario	**Timing of eruption**	**Eruption site**	**SRM**
SRM Volc Jan	1. January	Pinatubo (15° N, 120° E)	suspended
SRM Arc Jan	1. January	Katmai (58° N, 155° W)	suspended
SRM Arc July	1. July	Katmai (58° N, 155° W)	suspended

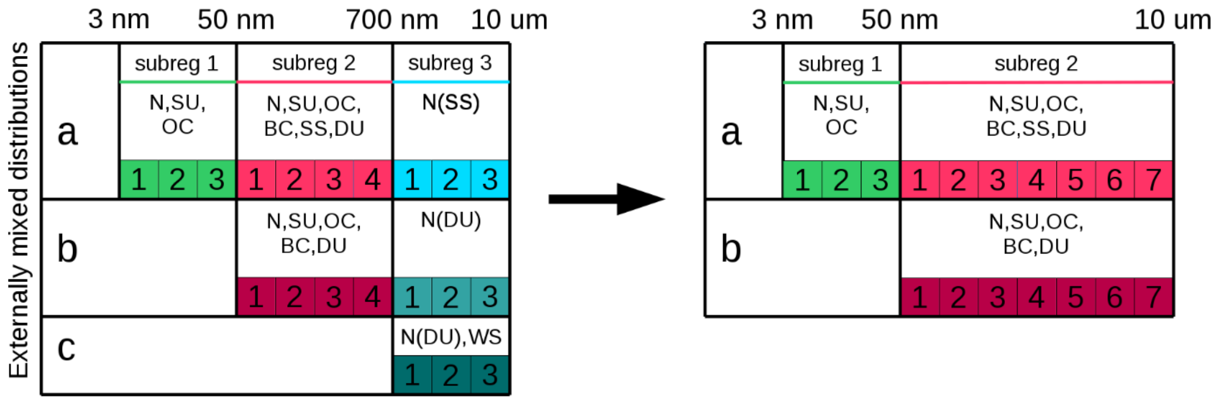

Figure 1. Particle size sections and chemical species in aerosol model SALSA. The left-hand figure illustrates the standard SALSA set-up. The rows ‘a’, ‘b’ and ‘c’ denote the externally mixed particle distributions. Within each distribution and subregion, N denotes number concentration and SU, OC, BC, SS and DU respectively sulfate, organic carbon, black carbon, sea salt and dust masses, which are traced separately. Within distribution ‘a’ and ‘b’ subregion 3, only particle number concentration is tracked, and all particles are assumed to be sea salt in distribution ‘a’ (N(SS)) and dust in distribution ‘b’ (N(DU)). In subregion 3 only number concentration (N(DU)) and water soluble fraction (WS) are traced. The numbers at the bottom of each subregion illustrate the size sections within that subregion. In our study, the third subregion is excluded and the second subregion is broadened to cover subregion 3 size sections (right-hand figure).

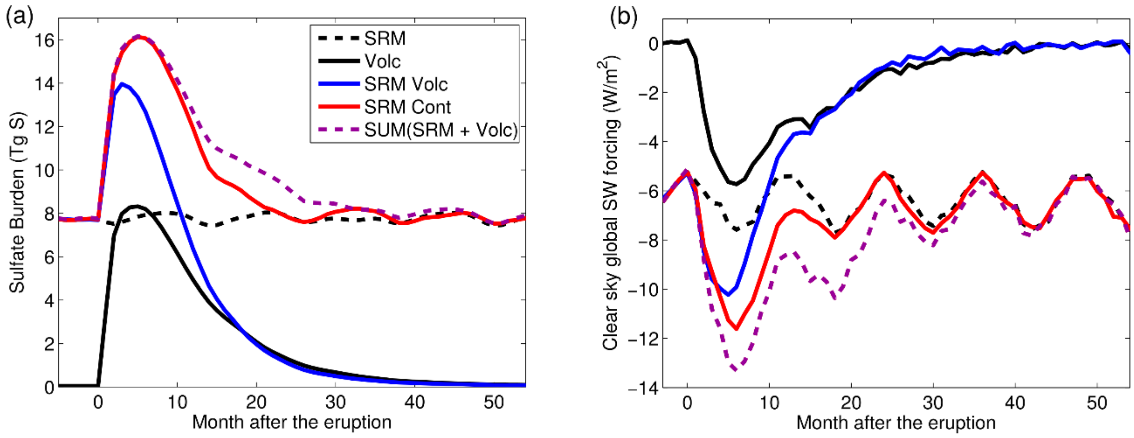

Figure 2. a) Stratospheric sulfate burden and b) global mean clear sky shortwave radiative forcing at the surface in the different scenarios. In addition, the dashed purple line represents the sum of SRM and Volc runs, and is shown for comparison.

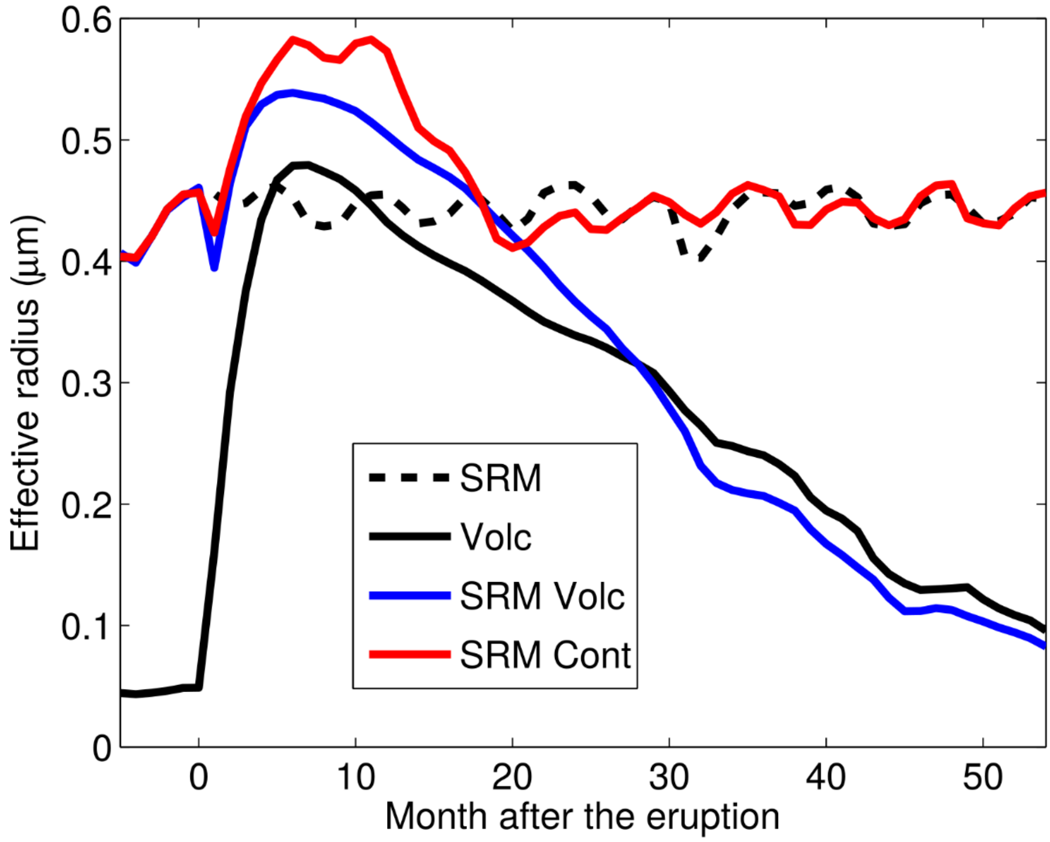

Figure 3. Mean effective radius in the different scenarios between 20°N and 20°S latitudes and between 20 - 25 km altitude levels.

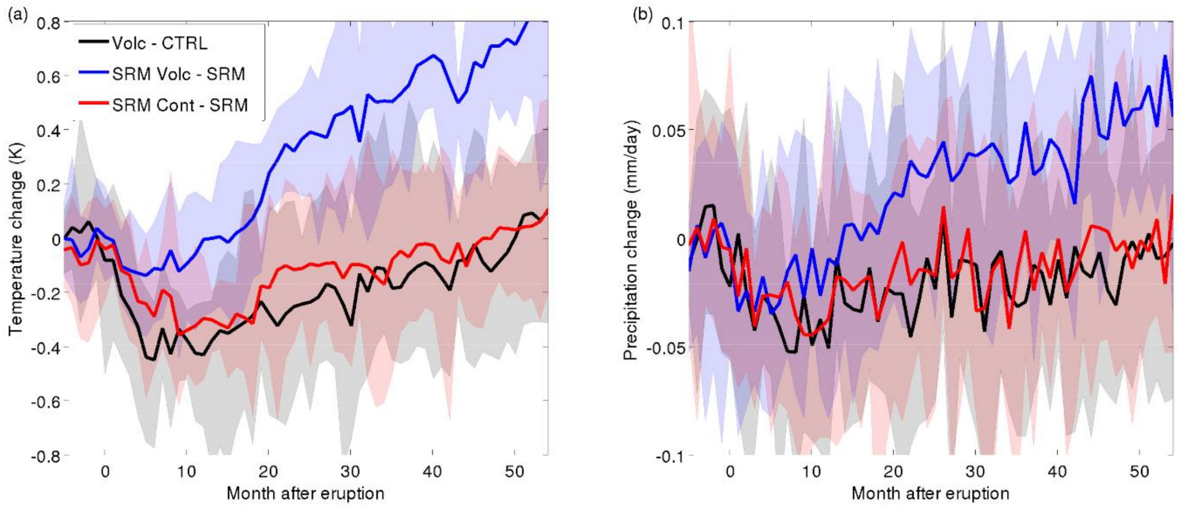

Figure 4. Global mean 2m a) temperature and b) precipitation changes after the volcanic eruption compared to the background condition (black line) and during solar radiation management (blue and red lines). Solid lines are mean values of the ten members of the ensemble simulations. The maximum and minimum values of the ensemble are depicted by shaded areas.

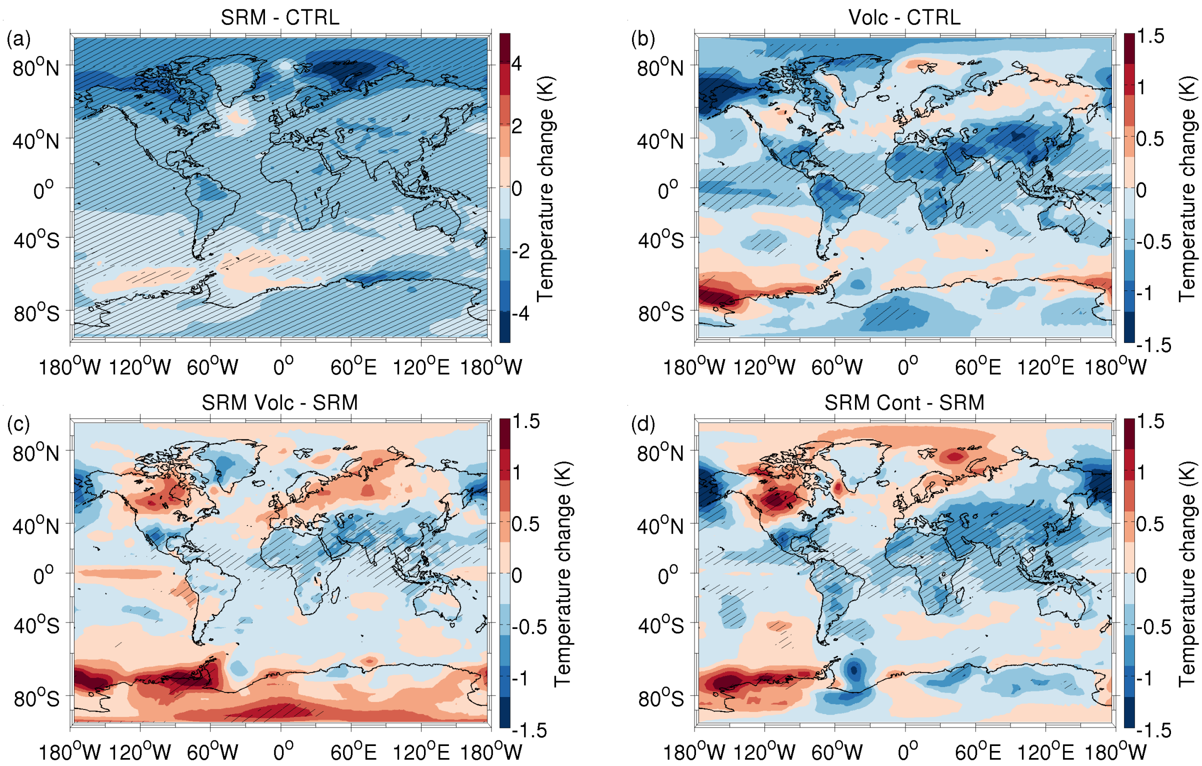

Figure 5. Ensemble mean change in annual mean 2-meter temperature. a) 50-year mean temperature change in SRM scenario. One-year-mean temperature change after the volcanic eruption in b) Volc, c) SRM Volc and d) SRM Cont compared to the pre-eruption climate (CTRL for SRM and Volc, and SRM for SRM Volc and SRM Cont). Hatching indicates a regions where the change of temperature is statistically significant at 95% level. Significance level was estimated using Student's unpaired t test with a sample of 10 ensemble member means for panels b-d and a sample of 50 annual means for panel a. Note different scale in panel a.

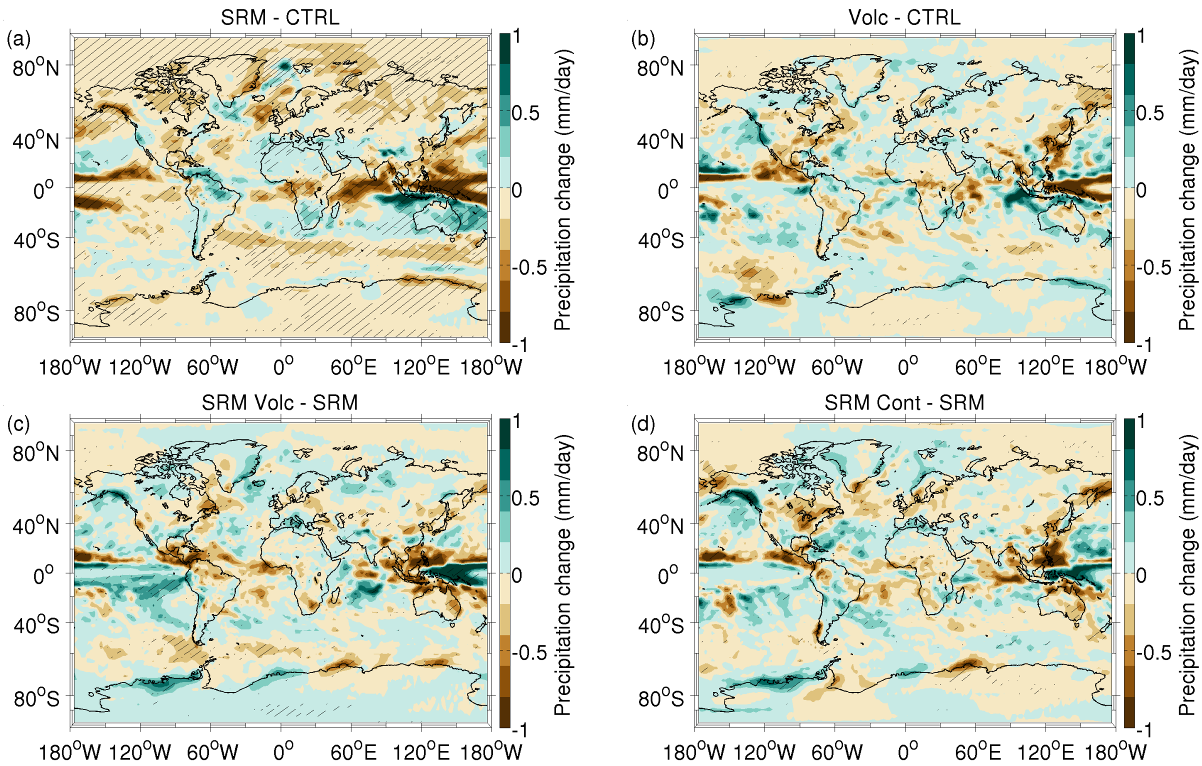

Figure 6. Ensemble-mean precipitation change in a) 50 year mean precipitation change in the SRM scenario. The change in one year mean precipitation after the volcanic eruption in b) Volc, c) SRM Volc and d) SRM Cont compared to the pre-eruption climate (CTRL for SRM and Volc, and SRM for SRM Volc and SRM Cont). Panels b-d show the one-year-mean temperature after the eruption. Panel a shows the mean over the corresponding one-year-periods as the other panels. Hatching indicates a regions where the change of precipitation is statistically significant at 95% level. Significance level was estimated using Student's unpaired t test with a sample of 10 ensemble member means for panels b-d and a sample of 50 annual means for panel a.

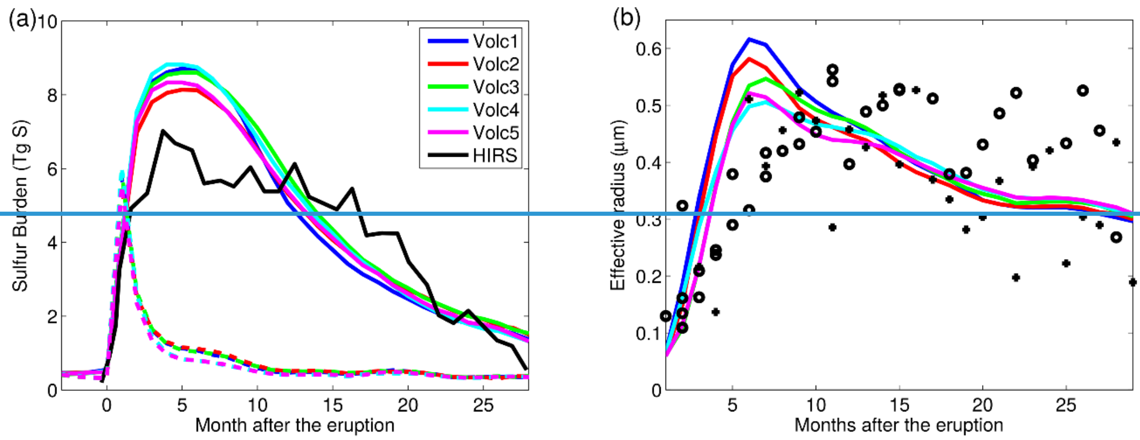

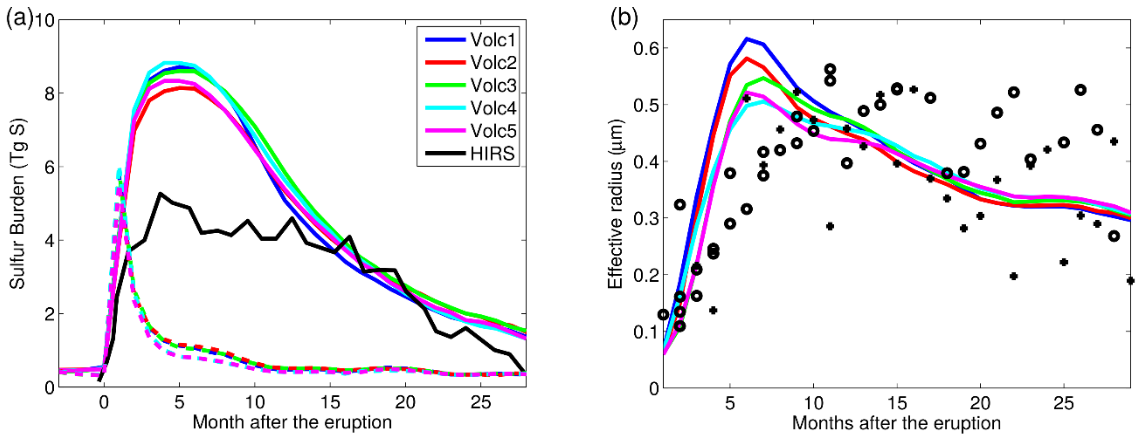

Figure A1. a) Global ~~stratospheric~~ SO_2 (dashed lines) and particulate sulfate (solid lines) burdens after a simulated volcanic eruption in July compared to sulfate observations from HIRS satellite after the 1991 Pinatubo eruption (black). b) Zonal mean effective radius at 53° N latitude after the simulated July eruption compared to lidar measurements at Laramie 41° N (dots) and Geestracht 53° N (crosses) after the Pinatubo eruption (Ansmann et al., 1997). In both panels the results are shown for altitude range 16 - 20 km. The different colored lines show results from the 5 members of the simulated ensemble (simulations Volc1,…, Volc5).

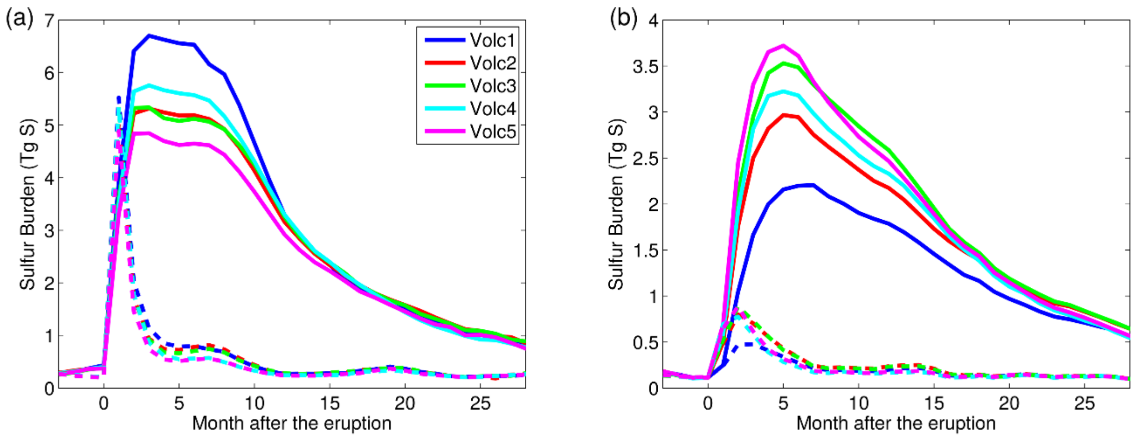

Figure A2. SO_2 (dashed lines) and sulfate (solid lines) burden after the eruption on a) northern hemisphere and b) southern hemisphere. Note different scale in Y-axes.

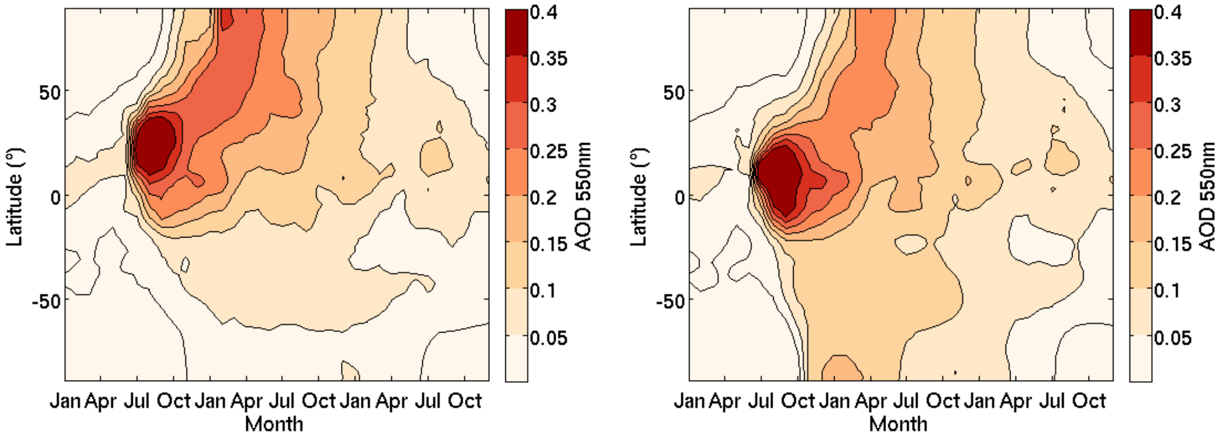

Figure A3. Zonal and monthly mean 550 nm aerosol optical depth after volcanic eruption in a) Volc1 simulation and b) Volc5 simulation

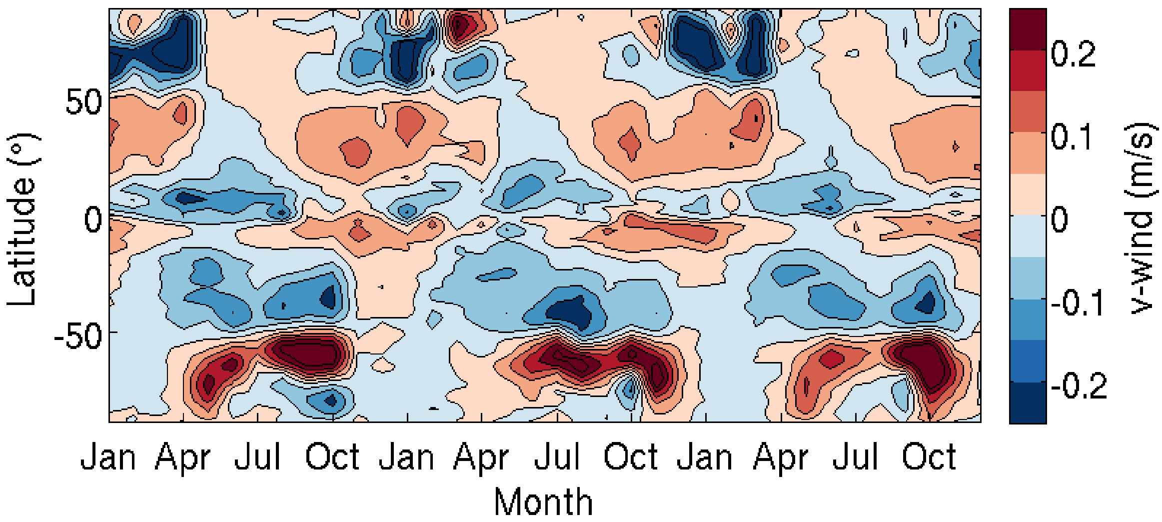

Figure B1. Merieodional wind components (positive values from south to north) at 25 km altitude in CTRL simulation with MAECHAM5-HAM-SALSA.

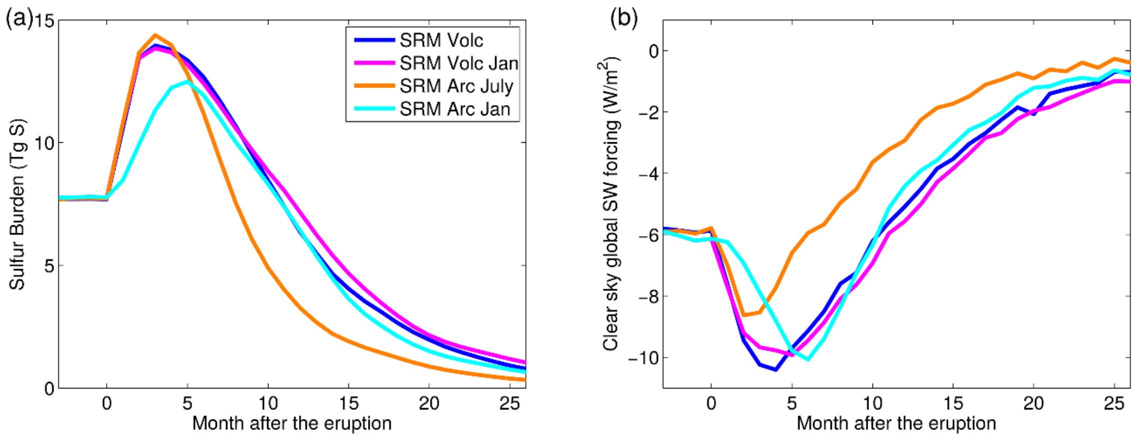

Figure B2. a) Stratospheric sulfate burden and b) global mean clear sky shortwave radiative forcing after the eruption in January (blue line) and July (magenta line) and Arctic eruption in January (cyan line) and July (orange line).